Department of Biomedical Engineering and Computational Science

Ionic mechanisms in mouse rod photoreceptor signaling

Frans Vinberg

A!

DOCTORAL DISSERTATIONS

Aalto University publication series
DOCTORAL DISSERTATIONS 67/2011

Ionic mechanisms in mouse rod photoreceptor signaling

Frans Vinberg

Doctoral dissertation for the degree of Doctor of Science in Technology to be presented with due permission of the School of Science for public examination and debate in Auditorium F239 at the Aalto University School of Science (Espoo, Finland) on the 21st of September 2011 at 12 noon.

Aalto University
School of Science
Department of Biomedical Engineering and Computational Science

Supervisor
Professor Ari Koskelainen

Instructor
Professor Ari Koskelainen

Preliminary examiners
Dr. Viktor Govardovskii, Russian Academy of Sciences, Russian
Dr. Michael Woodruff, University of California, USA

Opponent
Associate Professor Vladimir Kefalov, Washington University School of Medicine, USA

Aalto University publication series
DOCTORAL DISSERTATIONS 67/2011

ISBN 978-952-60-4235-0 (pdf)
ISBN 978-952-60-4234-3 (printed)
ISSN-L 1799-4934
ISSN 1799-4942 (pdf)
ISSN 1799-4934 (printed)

Aalto Print
Helsinki 2011

Finland

The dissertation can be read at http://lib.tkk.fi/Diss/

Publication orders (printed book):
frans.vinberg@aalto.fi

Aalto University

Abstract

Aalto University, P.O. Box 11000, FI-00076 Aalto www.aalto.fi

Author
Frans Vinberg

Name of the doctoral dissertation
Ionic mechanisms in mouse rod photoreceptor signaling

Publisher School of Science

Unit Department of Biomedical Engineering and Computational Science

Series Aalto University publication series DOCTORAL DISSERTATIONS 67/2011

Field of research Tfy-99 Biomedical Engineering

Manuscript submitted 14 June 2011 **Manuscript revised** 16 August 2011

Date of the defence 21 September 2011 **Language** English

☐ **Monograph** ☒ **Article dissertation (summary + original articles)**

Abstract

Photoreceptor cells are an example of biological transducer devices: they transform photon energy into an electrical signal and transmit it to higher-order neurons. Vertebrate photoreceptor cells can be categorized into two classes, rods and cones. The rod photoreceptors are extremely sensitive to light, whereas cones are faster than rods and can function under bright ambient illumination. The rod photoreceptor cell is a convenient model for studying modulation of physiological transduction and transmission processes because 1) the rod's natural input signal, light, can be applied quantitatively and 2) the absorption of only one or a few photons by the visual pigment molecules in the cell's outer segment is transformed into a measurable change of the rod's membrane potential (V_m). The gain of the photon-to-V_m conversion in rods is rapidly (in a fraction of a second) modulated by several ionic feedback mechanisms. The mechanisms involved in rod signal generation and feedback signaling were investigated in the present work by recording rods' electrical responses to light stimuli from intact mouse retinas with transretinal electroretinogram (ex vivo ERG).

Several negative feedback mechanisms that accelerate a rod's response recovery after light stimuli rely on the light-induced decline in the calcium ion (Ca^{2+}) concentration in the rod outer segment. Further, some voltage- and Ca^{2+} -dependent mechanisms in the rod inner segment plasma membrane modulate the gain of the photon-to-V_m conversion. In this thesis the specificity of the known Ca^{2+} signaling mechanisms, and Ca^{2+} dependency of the reaction that rate-limits the rod's recovery after bright stimuli were investigated. It was found that the transition metal ion Co^{2+} can mediate the known Ca^{2+} dependent negative feedback mechanisms in the rod outer segment, and that a certain minimum amount of Ca^{2+} is necessary in setting the physiological value of the speed of the rate-limiting recovery reaction. The role of the inner segment ionic channels in generating the rod ERG response was also elucidated. It was shown that the hyperpolarization activated (h) channels in the rod inner segment participate in the generation of a fast transient component that is evident in the rod ERG response to bright flashes. Instead, voltage-dependent Ca^{2+} channels or Ca^{2+} -activated potassium and chloride currents did not contribute to that component. Additionally, modulation of the direct electrical transmission between rods and cones was studied. The present work suggests that the electrical connection between rods and cones can be closed by light in the mouse retina.

Keywords photoreceptor, electrophysiology, electroretinogram, calcium signaling

ISBN (printed) 978-952-60-4234-3 **ISBN (pdf)** 978-952-60-4235-0

ISSN-L 1799-4934 **ISSN (printed)** 1799-4934 **ISSN (pdf)** 1799-4942

Location of publisher Espoo **Location of printing** Helsinki **Year** 2011

Pages 153 **The dissertation can be read at** http://lib.tkk.fi/Diss/

Aalto-yliopisto

Tiivistelmä

Aalto-yliopisto, PL 11000, 00076 Aalto www.aalto.fi

Tekijä
Frans Vinberg

Väitöskirjan nimi
Ioniohjatut mekanismit hiiren sauvasolussa

Julkaisija Perustieteiden korkeakoulu

Yksikkö Lääketieteellisen tekniikan ja laskennallisen tieteen laitos

Sarja Aalto University publication series DOCTORAL DISSERTATIONS 67/2011

Tutkimusala Tfy-99 Lääketieteellinen tekniikka

Käsikirjoituksen pvm 14.06.2011 **Korjatun käsikirjoituksen pvm** 16.08.2011

Väitöspäivä 21.09.2011 **Kieli** Englanti

☐ **Monografia** ☒ **Yhdistelmäväitöskirja (yhteenveto-osa + erillisartikkelit)**

Tiivistelmä

Näköaistinsolu toimii biologisena anturi- ja lähetinkomponenttina muuntaen fotonien energian sähköisiksi signaaleiksi, jotka se lähettää seuraaville hermosoluille. Selkärankaisten näköaistinsolut voidaan jakaa kahteen luokkaan, tappi- ja sauvasoluihin. Sauvasolut ovat erittäin herkkiä valolle soveltuen parhaiten hämärän ympäristön aistimiseen, kun vastaavasti tappisolut signaloivat sauvoja nopeammin ja kirkkaammassa ympäristössä. Sauvasolut soveltuvat hyvin fysiologisten signaalien vahvistus- ja lähetinominaisuuksien tutkimiseen kahdestakin syystä: 1) niiden luonnollista tulosignaalia (valo) voidaan syöttää hallitusti, ja 2) jo yksittäisen fotonin absorboituminen sauvasolun näköpigmenttiin tuottaa mitattavissa olevan muutoksen solun kalvojännitteessä (V_m). Vahvistusta, jolla sauvasolu muuntaa fotonin energian V_m-signaaliksi, voidaan säätää nopeasti (sekunnin murto-osassa) useilla ionien ohjaamilla mekanismeilla. Tässä työssä tutkittiin joitakin näistä mekanismeista eristetyn verkkokalvon elektroretinogrammitekniikalla (ERG).

Sauvasolujen valostimulaation aiheuttaman sähköisen vasteen (valovaste) katkaisunopeutta säädellään usealla negatiivisella takaisinkytkentämekanismilla, joita ohjaavat kalsiumionin (Ca^{2+}) konsentraatiomuutokset sauvasolun ulkojäsenessä valovasteen aikana. Fotoni-V_m muunnon vahvistusta muokataan edelleen sauvasolun sisäjäsenen solukalvossa sijaitsevien Ca^{2+}- ja jänniteherkkien kanavien avulla. Tässä väitöskirjassa tutkittiin Ca^{2+}-signalointimekanismien spesifisyyttä sekä sauvan valovasteen palautumisnopeutta rajoittavan reaktion kalsiumriippuvuutta kirkkaan valostimuluksen jälkeen. Tulosten pohjalta voitiin päätellä, että 1) siirtymämetalli-ioni koboltti (Co^{2+}) pystyy välittämään tunnettuja kalsiumriippuvia negatiivisia takaisinkytkentämekanismeja sauvasolun ulkojäsenessä, ja 2) tietty määrä kalsiumia tarvitaan asettamaan valovasteen katkaisun nopeutta rajoittavan reaktion fysiologinen kinetiikka. Tässä työssä selvitettiin myös kuinka sisäjäsenen solukalvon ionimekanismit näkyvät kirkkaan valopulssin aiheuttamassa sauvojen ERG-vasteessa. Tulokset osoittivat, että solukalvon hyperpolarisaation kautta aktivoituvat (h) kanavat sauvasolun sisäjäsenessä osallistuvat kirkkaan valopulssin aiheuttaman nopean transientin ERG-signaalikomponentin syntyyn. Toisaalta näytettiin, että jänniteherkät kalsiumkanavat tai kalsiumohjatut kalium- tai kloridivirrat eivät näy kyseisessä komponentissa. Lisäksi tutkittiin sauvojen ja tappien välisen suoran sähköisen yhteyden modulaatiota. Tulokset viittaavat siihen että tämä sähköinen yhteys voidaan sulkea valon avulla.

Avainsanat näköaistinsolu, sähköfysiologia, elektroretinogrammi, kalsiumsignalointi

ISBN (painettu) 978-952-60-4234-3 **ISBN (pdf)** 978-952-60-4235-0

ISSN-L 1799-4934 **ISSN (painettu)** 1799-4934 **ISSN (pdf)** 1799-4942

Julkaisupaikka Espoo **Painopaikka** Helsinki **Vuosi** 2011

Sivumäärä 153 **Luettavissa verkossa osoitteessa** http://lib.tkk.fi/Diss/

Preface

This thesis project has been conducted at Aalto University (former University of Technology), Department of Biomedical Engineering and Computational Science (BECS). I am grateful to the previous and current heads of department: emeritus Professor Toivo Katila, Professor Risto Ilmoniemi and Professor Jouko Lampinen for providing facilities and inspiring environment for research. Also, the financial support by the Finnish Academy of Science and the International Doctoral Programme in Biomedical Engineering and Medical Physics (iBioMEP) is acknowledged.

I want to express my gratitude to my supervisor Professor Ari Koskelainen who introduced me to the world of photoreceptor electrophysiology. His experience in experimental research and readiness to use his time for interesting discussions about science and other issues has been invaluable. I want to thank Professor Kristian Donner, Dr. Simo Hemilä and emeritus Professor Tom Reuter whose wide knowledge has inspired me along the journey. I also want to express my gratitude to Magnus Lindström, the organizer of the annual vision seminar Visionarium. These meetings have provided a relaxed atmosphere for sharing information between scientists in the extremely beautiful surroundings of Tvärminne.

I thank all my present and former co-workers in the Biophysics group. I am especially grateful to Dr. Hanna Heikkinen who has helped me in many ways during the course of this project, in particular I want to thank for her invaluable contribution to the writing process of this thesis. I also want to thank Dr. Soile Nymark, Dr. Hanna Mäki, Elina Sahala, Teemu Turunen, Marja Pitkänen and Janne Räsänen for their company and contribution to many of the experiments related to this thesis. Discussions about life and science with Pia Saarinen, Dr. Johan Pahlberg, Dr. Petri Ala-Laurila, Rauli Albert, Dr. Bertel Kommonen, Markku Kilpeläinen and Dr. Viljami Salmela have also been very pleasant.

I appreciate the expert comments of the preliminary examiners Dr. Michael Woodruff and Dr. Viktor Govardovskii on the manuscript of this thesis.

Finally, I want to express my deepest gratitude to my closest. The love and support by my mom and dad has always been unconditional and they have supported and guided me along my life journey. Noora, thank you for your love and the patience you have showed to me also during the difficult moments of this thesis project.

Contents

List of publications

The present thesis is based on the following four publications referred to by their Roman numerals in the text:

I F. Vinberg, S. Strandman and A. Koskelainen (2009). Origin of the fast negative ERG component from isolated aspartate-treated mouse retina. *Journal of Vision*, **9**: 9-17

II F. Vinberg and A. Koskelainen (2010). Calcium sets the physiological value for the dominant time constant of the saturated mouse rod photoresponse recovery. *PLoS ONE*, **5**: e13025

III F. Vinberg and A. Koskelainen (2011). Cobalt (Co^{2+}) can mediate dynamic feedback signals driven by calcium (Ca^{2+}) sensor molecules in mouse rod photoreceptors. Aalto University publication series, SCIENCE + TECHNOLOGY, 12/2011, ISSN 1799-490X, 28 pages

IV H. Heikkinen, F. Vinberg, S. Nymark and A. Koskelainen (2011). Mesopic background lights enhance dark-adapted ERG cone flash responses in the intact mouse retina: a possible role for gap junctional decoupling. *Journal of Neurophysiology*, **105**: 2309-2318

Author's contributions

The author has had a significant role in all aspects of the research presented in papers I – IV. He has refined the experimental protocols in recording electroretinogram (ERG) from isolated mouse retinas. He is the first author in papers I - III. He has done all the experimental work (except the synthesis of dimethonium in paper I), data analysis and figure preparation for papers I - III. He has written the first draft of the manuscripts and participated actively in the writing of the final versions of papers I – III. He has done a substantial part of the experiments and participated actively in writing of the manuscript for paper IV.

List of abbreviations and symbols

V_m	membrane potential
GTP	guanosine triphosphate
GDP	guanosine diphosphate
GPCR	G-protein coupled receptor
Rh	rhodopsin
G_t	transducin
R*	active rhodopsin
Φ	flash strength
cGMP	cyclic guanosine monophosphate
cAMP	cyclic adenosine monophosphate
ATP	adenosine triphosphate
GC	guanylyl cyclase
ROS	rod outer segment
CNG channel	cGMP-gated (or cyclic nucleotide-gated) channel
J_{cG}	current through CNG channels
NCKX	Na^+/ Ca^{2+}, K^+ exchanger
J_{ex}	current through NCKXs
PDE	phosphodiesterase
E*	active phosphodiesterase
A	amplification factor
τ_D	dominant time constant of saturated flash photoresponse recovery
τ_E	average life time of E*
τ_R	average lifetime of R*
GRK	rhodopsin kinase
Arr	arrestin
Rec	recoverin
RGS9	membrane-associated GTPase accelerating protein complex
HCN channel	hyperpolarization-activated cyclic nucleotide-modulated channel
Kx channel	depolarization-activated non-inactivating potassium channel
BK channel	Ca^{2+} -activated potassium channel
PMCA	plasma membrane Ca^{2+} ATPase
E_r	reversal potential
ERG	electroretinogram
fast PIII	photoreceptor component of ERG

1. Introduction

The central nervous system (CNS) receives information from the sensory neurons of the peripheral nervous system and controls the movement and behavior of individuals. Of the senses vision is considered the most important for many species, including humans. Our ability to follow quickly moving objects under daylight, and on the other hand to adapt to see distant stars 10^{10} –fold dimmer than the ambient illumination we encounter during a sunny day, is impressive. Performing such versatile functions sets high demands for the system that senses, transmits and processes the visual signals. What's more, already the transduction of the input signal, light, into an electrical signal by the sensory neurons must be effectively regulated to preserve the relevant information about the visual scene under varying mean light levels.

Neurons use ionic mechanisms both in their membranes and inside the cell to rapidly adapt their function in response to some external stimuli, contrasting the slower modulation through e.g. hormonal pathways. The neural network of the vertebrate retina is specialized to receive information about the light distribution around the individual and to transmit it to other parts of the brain. The requirement for the visual system to function over a wide range of light intensities is partly met by using two classes of photoreceptor cells, rods and cones. The rods are more sensitive to light and can function at very low light levels, whereas the cones are less sensitive to light but are faster than rods and can function under bright ambient illumination. Yet the wide range of the natural input stimuli requires substantial gain control also within individual photoreceptors. The photon absorption by the visual pigment molecules in a photoreceptor leads to a transient decrease of an inward cationic current in the photoreceptor's plasma membrane through a biochemical cascade called *phototransduction*, the gain of which is controlled with several intricate feedback mechanisms. Because a proportion of the light-sensitive cationic current is carried by calcium ions (Ca^{2+}) into the photoreceptor and the extrusion of Ca^{2+} through the plasma membrane continues under illumination, $[Ca^{2+}]$ in the photoreceptors declines as a consequence of light stimulation. This acts as an important signal regulating the gain of phototransduction through several intracellular Ca^{2+} sensor proteins. The gain of the photon-V_m conversion is further controlled by voltage-dependent ionic currents through the plasma membrane. Although rod-based vision has been optimized for high sensitivity at the expense of temporal resolution, also rods have de-

veloped strategies for faster signaling when the ambient light level increases. As an example, rods' signal transmission can switch between the slower primary rod pathway and the faster cone pathways by modulating the conductance of the electrical connection through the gap junctions between rods and cones (Ribelayga *et al.*, 2008; Ribelayga & Mangel, 2010).

In this thesis the rod photoreceptor cell was used as a model system to study the mechanisms that regulate the gain of a biological transducer system and its temporal signal transmitter properties. The rod is a convenient system to study such mechanisms, because the natural input signal, light, is easily conveyed to the photoreceptor cells in a controlled way, and the high inherent gain of the transduction generates large output responses that can be recorded with high precision. This thesis investigates the role of voltage-dependent currents and Ca^{2+} signaling mechanisms that modulate the gain of the photon-V_m relationship of the mouse rods. Also, light-dependent modulation of the gap junction conductance between rods and cones controlling the transmission speed of rod-originated signals in the mammalian retina is studied.

2. Review on literature

2.1 Phototransduction and ionic mechanisms in rod outer segment

The first step in photoreceptor cell activation is the conversion of the light information into an electrical signal in the process called *phototransduction*. In vertebrates the phototransduction takes place in the outer segment of a ciliary rod or cone photoreceptor cell (ROS or COS, respectively). There, the absorption of a photon by a visual pigment molecule is transformed into hyperpolarization of the plasma membrane potential (V_m) via a G-protein-mediated signaling (GPCR signaling) process. The phototransduction in rods represents the best known GPCR signaling cascade, and is here reviewed in Figure 1 (Yau & Hardie, 2009). Historically, most of the knowledge about phototransduction has accumulated from the studies on cold-blooded vertebrates (mostly anurans and salamanders) but now also mammalian, and especially the mouse (*Mus musculus*) rod phototransduction (Fu & Yau, 2007) is very thoroughly understood (for a historical review, see Luo *et al.*, 2008).

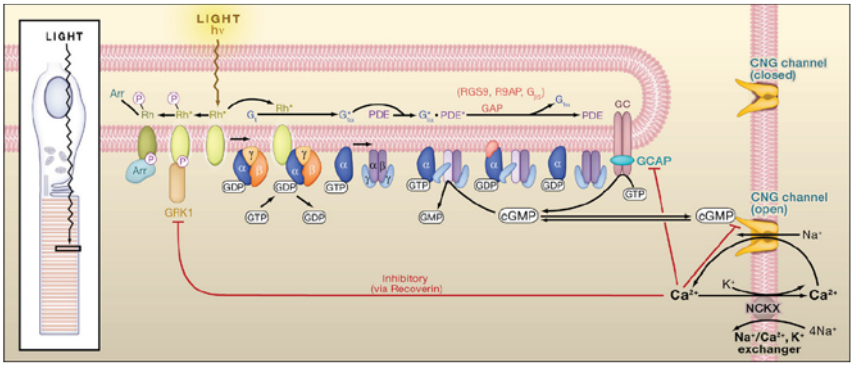

Figure 1 Scheme for the rod phototransduction shown in one disc membrane with the nearby plasma membrane. Reprinted with permission from Yau & Hardie (2009), © Elsevier Ltd.

2.1.1 Activation of phototransduction cascade by light leads to a decrease in inward cationic current (J_{cG})

One of the special features of the rod GPCR signaling cascade is the high molecular amplification, which is realized through a series of biochemical reactions. The visual pigment molecules in rods, rhodopsins (Rh), are embedded in the disc membranes that are separated from the ROS plasma membrane (see Figure 1). Rh is activated upon a photon absorption, and the active form of a rhodopsin, R*, can activate several G proteins (transducins, G_ts) while diffusing laterally in

the disc membrane. Binding of R* to G_t favors the exchange of GTP for GDP in the α-subunit of transducin, and consequently the active $G_{t\alpha\text{-}GTP}$ (=G_t*) detaches from the β- and γ-subunits of G_t. Each G_t* can activate one effector protein phosphodiesterase (PDE6), which then starts to hydrolyse cGMP molecules, leading to a decrease in [cGMP] in ROS. The reduction of cGMP concentration closes cGMP-gated channels (CNG channels) in the ROS plasma membrane (Fesenko *et al.*, 1985).

The CNG channel is the only cationic channel type present in ROS. It is permeable to most mono- and divalent cations (Yau *et al.*, 1981; Menini *et al.*, 1988), and in a physiological ionic environment (and physiological membrane potential) the CNG channel current (J_{cG}) is negative (i.e. inward). *Ca.* 80 – 90 % of J_{cG} is carried by sodium (Na^+) and 10 - 15% by calcium (Ca^{2+}) with a small additional contribution from Mg^{2+} (Nakatani & Yau, 1988b). In darkness J_{cG} is about -20 pA in the mouse rod (reviewed in Pugh, Jr. & Lamb, 2000). In mouse the activation of a single rhodopsin molecule closes ~5% of the CNG channels that are open in darkness, causing ~1 pA change of J_{cG} (Chen *et al.*, 1995b). The decrease in inward J_{cG} decelerates the inflow of Ca^{2+} and consequently the cytosolic Ca^{2+} concentration ($[Ca^{2+}]_i$) is lowered, because the Na^{2+}/Ca^{2+}, K^+ exchangers (NCKX1s) in the ROS plasma membrane continue to extrude Ca^{2+}. The decrease in $[Ca^{2+}]_i$ is an important feedback signal to phototransduction shut-off mechanisms that will be discussed in the following sections.

2.1.2 Cascade shut-off and recovery of J_{cG}

In order to maintain the dark-adapted J_{cG} or to restore its pre-stimulus value, cGMP has to be synthesized. In ROS cGMP is produced from GTP by guanylyl cyclases (GCs, for a review see Pugh, Jr. *et al.*, 1997). The light-induced decrease of free $[Ca^{2+}]_i$ in ROS increases the GC activity and thus accelerates the restoration of [cGMP]. This has been shown to be a Ca^{2+} feedback mechanism of particular importance for the rod phototransduction (see below).

The light-induced activity of PDE must be quenched in order to regain the rod's responsiveness. This requires inactivation of both active rhodopsin (R*) and active phosphodiesterase (E*) molecules. Both of these inactivation processes are controlled by specialized protein molecules discussed in 2.1.3 and 2.1.4. Here a phenomenological model is adopted. It describes the amount of E*s by assuming that both the R* and the E* inactivation reactions obey a first-order exponential decay with average lifetimes τ_{ND} and τ_D (Nikonov *et al.*, 1998) giving

$$E^*(t) = \left\{ \Phi \exp\left[-\frac{t}{\tau_{ND}} \right] \right\} * \left\{ \nu_E \exp\left[-\frac{t}{\tau_D} \right] \right\}, \qquad (1)$$

where Φ is the amount of R* activated by a flash of light (impulse input), ν_E is the rate of E* production by a single R* (in s^{-1}), and $*$ denotes a convolution operator. The dominant time constant, τ_D (Pepperberg *et al.*, 1992), is the longer and the non-dominant time con-

stant τ_{ND} is the shorter of the time constants. The τ_D is important in determining the kinetics of photoresponse recovery, and the determination of τ_D by electrophysiological recordings will be discussed later in this thesis.

Data from amphibian and mouse rods strongly indicates that τ_D corresponds to the lifetime of E* (=τ_E), which is ~0.2 s at 37°C in the mouse rod (Krispel et al., 2006, but see Doan et al., 2009). Earlier data from amphibians suggested that τ_D is not modulated by light (Nikonov et al., 2000), but recent results on mouse rods suggest that background light might shorten the lifetime of E* in mammalians (Woodruff et al., 2008). Most experimental evidence indicate that in WT mouse rods the average lifetime of R* (τ_R) is shorter than τ_E. Experiments on transgenic mice and modeling studies suggest that τ_R is less than 50 ms in the mouse rod at 37°C (Chen *et al.*, 2010a; Burns & Pugh, Jr., 2010; Gross & Burns, 2010). However, this view has been challenged by Doan and others (Doan et al., 2009), whose data and simulations suggest that τ_R is τ_D (≈ 0.4 s).

2.1.3 Negative feedback mechanisms of rod phototransduction

Exposure of photoreceptors to light reduces their gain of the R*-to-V_m conversion. Much of this regulation is implemented by negative feedback mechanisms acting on the phototransduction reactions that control the recovery kinetics of J_{cG} after light stimulus. In rods, three negative feedback mechanisms have been described: (1) acceleration of cGMP synthesis by GCs (Koch & Stryer, 1988; Mendez *et al.*, 2001Peshenko & Dizhoor, 2004), (2) shortening of the R* lifetime (Matthews *et al.*, 2001; Makino *et al.*, 2004), and (3) increase of the affinity of the CNG channels for cGMP (Hsu & Molday, 1993; Chen *et al.*, 2010b). Ca^{2+} is thought to play an important role in these feedback mechanisms (see below), and the following sections of this chapter (2.1.3) will concentrate to review how the light-induced change of $[Ca^{2+}]_i$ in the rod outer segment controls the feedback mechanisms (1) and (2). The effect of mechanism (3) is quite modest on the electrical responses of mammalian rods (Rebrik & Korenbrot, 2004; Chen *et al.*, 2010b) and will not be discussed in this thesis.

Ca^{2+} is the internal transmitter of the negative feedback mechanisms in the rod outer segment

The role of Ca^{2+} in the rod phototransduction was investigated already before the molecular mechanisms in ROS were resolved by 1) modulating extracellular $[Ca^{2+}]$, 2) slowing the changes of $[Ca^{2+}]_i$ by intracellularly applied Ca^{2+} buffers (BAPTA, Torre *et al.*, 1986) or 3) inhibiting the plasma membrane Ca^{2+} fluxes (Matthews *et al.*, 1988; Nakatani & Yau, 1988a). Intracellular and extracellular recordings have shown that the rod membrane potential depolarizes in response to lowered $[Ca^{2+}]_o$ and hyperpolarizes in response to elevated $[Ca^{2+}]_o$ in darkness (Hagins *et al.*, 1970; Brown & Pinto, 1974). However, in bright light the rod membrane potential seemed to be independent of $[Ca^{2+}]_o$. Thus, the saturated *photoresponse* amplitude increases in low Ca^{2+} and decreases in high Ca^{2+} (Brown & Pinto, 1974). A similar effect of Ca^{2+} can be seen in the CNG channel current which increases in low Ca^{2+} and decreases in high Ca^{2+} conditions (Yau *et al.*, 1981).

Calcium acts both externally and internally on ROS. The external effect comes through a direct decrease of the single CNG channel conductance. If $[Ca^{2+}]_o$ is lowered from 1 mM to < 10^{-8}, the single channel conductance is increased 3- to 4-fold (Haynes *et al.*, 1986; Stern *et al.*, 1987; Lamb & Matthews, 1988). Also inside the ROS, Ca^{2+} acts to decrease J_{cG} by inhibiting the production of cGMP, and thus by decreasing the open probability of the CNG channels. E.g. if $[Ca^{2+}]_o$ is lowered from 1 mM to 10^{-8} M, the internal effects account for at least a 4- to 5-fold increase of the CNG channel current (Lamb & Matthews, 1988).

The most conclusive evidence for identifying Ca^{2+} as the internal messenger of the negative feedback mechanisms came from the experiments that slowed or prevented the changes of $[Ca^{2+}]_i$ in the ROS. These experiments showed that if $[Ca^{2+}]_i$ was clamped to the same level as in darkness (= $[Ca^{2+}]_{dark}$), the rods did not exhibit the initial recovery of J_{cG} after exposure to constant background light, a phenomenon that is normally present when free $[Ca^{2+}]_i$ is free to change. Also the acceleration of flash photoresponse recovery caused by light stimulation was diminished or even abolished in the rods whose $[Ca^{2+}]$ in ROS was clamped to physiological $[Ca^{2+}]_{dark}$ (Fain *et al.*, 1989; Matthews, 1995). Further, some of the effects of background light could be accurately mimicked by decreasing $[Ca^{2+}]$ (Matthews, 1995). Recordings from cells, in which the changes of $[Ca^{2+}]_i$ had been slowed by increasing intracellular calcium buffering (by introducing the calcium buffer BAPTA into the rods), showed decelerated flash response recovery (Torre *et al.*, 1986), consistent with the data obtained by manipulating the Ca^{2+} fluxes across the ROS plasma membrane.

Although most of the data indicated that the decrease of $[Ca^{2+}]_i$ in ROS acts as a negative feedback signal, some effects of low $[Ca^{2+}]_o$ exposure remained controversial: The exposure of a rod to very low $[Ca^{2+}]_o$ makes flash photoresponses slower, which is just the opposite to what the light-induced decline of $[Ca^{2+}]_i$ does. Also, rods become less sensitive to light flashes and the CNG channel current increases only transiently before declining to a much lower value compared to that in physiological $[Ca^{2+}]_o$ (Lipton *et al.*, 1977; Yau *et al.*, 1981; Bastian & Fain, 1982; Hodgkin *et al.*, 1984; Matthews, 1995). It was suggested that these anomalies might arise indirectly from the increased [cGMP] and thus J_{cG}, or from the accumulation of Na^+ into the ROS (Yau *et al.*, 1981; Hodgkin *et al.*, 1984; Matthews, 1995). However, the contributions of these effects on the response properties of rods under low Ca^{2+} conditions are still not completely understood. The reasons for the slower response kinetics in very low (~10^{-8} M) $[Ca^{2+}]_o$ were investigated in papers II and III.

Regulation of $[Ca^{2+}]$ in the rod outer segment

The $[Ca^{2+}]$ in the rod outer segment in darkness is mainly set by a large influx and outflow of Ca^{2+} through the CNG channels and NCKXs in the ROS plasma membrane, respectively (for a review, see Schnetkamp, 1995a). The steady state concentration of free Ca^{2+} in the mouse ROS ($[Ca^{2+}]_i$) is ~250 nM in darkness and it rapidly de-

clines to ~20 - 50 nM as response to bright light that turns off the inflow of Ca^{2+} by closing the CNG channels (Woodruff *et al.*, 2002; Woodruff *et al.*, 2007). The total $[Ca^{2+}]$ in ROS ($[Ca^{2+}]_T$) is, however, much larger, because the major part of the intracellular calcium is bound to buffers and sequestered into internal stores. The Ca^{2+} buffers also act to decrease the rate of change in the free $[Ca^{2+}]_i$ and this has a significant effect on Ca^{2+} dynamics in ROS. The calcium-sensor protein recoverin is thought to contribute most to the buffering capacity ($B_{Ca} = d[Ca^{2+}]_T/d[Ca^{2+}]_i$, see 2.1.5) in the rod outer segment (Pugh, Jr. & Lamb, 2000; Makino *et al.*, 2004). Under certain circumstances also the release of Ca^{2+} from and sequestration of Ca^{2+} into internal stores (e.g. intradiscal space in ROS) might contribute to Ca^{2+} homeostasis and dynamics (see e.g. Kaupp *et al.*, 1979; Knopp & Rüppel, 1996; Matthews & Fain, 2001).

The rate of Ca^{2+} inflow in darkness can be inferred from the fraction of Ca^{2+} current through the CNG channels which in the mouse ROS is ~3 pA (15% of the CNG channel current), translating into inflow of ca. 6×10^6 Ca^{2+} ions per second through the open CNG channels. This inflow must be balanced by an equal rate of extrusion by NCKXs. The extrusion of Ca^{2+} against its electrochemical gradient relies on the movement of sodium and potassium along their electrochemical gradients. In one extrusion cycle 4 Na^+ ions are exchanged for one K^+ and one Ca^{2+} (Cervetto *et al.*, 1989). When all the CNG channels are closed, the only current-carrying mechanism in the ROS plasma membrane seems to be NCKX. Since the NCKX is electrogenic, it creates an inward current (J_{ex}). This current can be measured, and it has been shown to obey the Michaelis relation with respect to $[Ca^{2+}]_i$ (Cervetto *et al.*, 1989). The experimental data from amphibian rods indicates that the half activation $[Ca^{2+}]_i$ is ~1.5 μM (K_{ex}, reviewed in Pugh, Jr. & Lamb, 2000). Since the free $[Ca^{2+}]_i$ in the mouse ROS is always much smaller than K_{ex} in physiological conditions, the relation between J_{ex} and $[Ca^{2+}]_i$ is nearly linear (see Eq. (4) in 2.1.5). The stoichiometry of the exchanger indicates that in bright light $[Ca^{2+}]_i$ should decline below 1 nM (Cervetto *et al.*, 1989). However, it is believed that the ROS can maintain > 10 nM free $[Ca^{2+}]_i$ in mouse and other vertebrates (Schnetkamp, 1995b), although the mechanism preventing the $[Ca^{2+}]_i$ from dropping below 10 nM remains to be clarified.

Ca^{2+} -feedback on guanylyl cyclase activity

The most important feedback mechanism in the rod phototransduction is thought to be the acceleration of the GC activity as a response to the light-induced decline of $[Ca^{2+}]_i$ in the rod outer segment. Modulation of the GC activity accelerates the recovery of the rod's J_{cG} after light stimulus and extends the range of background illumination over which rods can operate (Mendez *et al.*, 2001; Chen *et al.*, 2010b). The biochemical data and studies with truncated and intact rod photoreceptors indicate that the GC activity increases 5-20 –fold in bright light (i.e. in low $[Ca^{2+}]_i$) compared to darkness (high $[Ca^{2+}]_i$) (Koch & Stryer, 1988; Cornwall & Fain, 1994; Koutalos *et al.*, 1995; Mendez *et al.*, 2001; Peshenko *et al.*, 2011). In the vertebrate rod,

cGMP is produced from GTP by two types of membrane-bound GCs (for review, see Pugh, Jr. *et al.*, 1997). The maximal rate of cGMP synthesis by GCs (when $[Ca^{2+}]_i$ is low) in the rod outer segment (= α_{max} in μMs^{-1}) has been measured experimentally only in a few studies. Koutalos and others (Koutalos *et al.*, 1995) were able to measure it from truncated salamander ROSs, yielding 25 μMs^{-1} (at nominal 0 Ca^{2+} and 1.6 mM $[Mg^{2+}]$). A very recent study indicates that in mouse rods α_{max} might be significantly larger, ~600 μMs^{-1} (Peshenko *et al.*, 2011). Although biochemical studies do not give absolute values for the GC activity in *in vivo* conditions, they can extract information about the Ca^{2+} sensitivities of GCs. Many of these studies give values for the half-activation concentration of Ca^{2+} (K_C) and co-operativity (Hill coefficient, n_C) that are similar to those inferred from functional studies on intact photoreceptors. There is some variability between different investigations, but the K_C appears to be between 100 and 200 nM and n_C between 2 and 3 (reviewed in Pugh, Jr. & Lamb, 2000).

Regulation of the rate of cGMP synthesis by $[Ca^{2+}]_i$ in rods is realized through guanylyl cyclase activating proteins (GCAP1 and GCAP2, Gorczyca *et al.*, 1994; Dizhoor *et al.*, 1995) which belong to the family of the EF –hand Ca^{2+}-sensor proteins (see 2.2.3). In darkness when $[Ca]_i$ is high, three of the four Ca^{2+} binding sites are occupied with Ca^{2+} and the GCAPs cannot activate GC. When the $[Ca^{2+}]_i$ declines after a light stimulus, Ca^{2+} ions dissociate from the binding sites making the GCAPs guanylyl cyclase activators (Lolley & Racz, 1982; Koch & Stryer, 1988; Gorczyca *et al.*, 1994; Dizhoor *et al.*, 1995).

Ca^{2+} -feedback on R inactivation*

Active rhodopsin is inactivated in a sequence of processes. First, multiple phosphorylations of R* by rhodopsin kinase (GRK1) are thought to gradually decrease the catalytic activity of R* on transducin (G) and to increase the affinity of R* to arrestin (Arr1), leading to a complete deactivation of R* when Arr1 binds to R* (Wilden *et al.*, 1986; Xu *et al.*, 1997; Chen *et al.*, 1999). The Ca^{2+} -dependent modulation of the R* lifetime is thought to be mediated by the Ca^{2+} sensor protein recoverin. Kawamura (Kawamura, 1993) showed biochemically that recoverin (or S-modulin) lengthens the R* lifetime in the presence of high $[Ca^{2+}]$. Consistently, recoverin-knockout mice show faster recovery kinetics for dim flashes and especially for saturated rod photoresponses compared to wild-type mice (Makino *et al.*, 2004). The physiological role of recoverin in modulating the R* lifetime was highlighted in a recent study by Chen and others (Chen *et al.*, 2010a). They generated a transgenic mouse in which R* deactivation was the rate-limiting reaction of the rod flash response recovery, facilitating the investigation of τ_R. It was shown that the lifetime of R* was modulated by background light, but if recoverin was knocked out this modulation was abolished. The present view is that in darkness, when $[Ca^{2+}]_i$ is high, recoverin with two Ca^{2+} bound is attached to GRK1 and prevents it from phosphorylating rhodopsin. When $[Ca^{2+}]_i$ declines after light stimulus, Ca^{2+} ions dissociate from recoverin

which then detaches from GRK1. Subsequently, the free GRK1 molecules can phosphorylate and thereby deactivate R* (Chen *et al.*, 1995a; Klenchin *et al.*, 1995; Ames *et al.*, 2006).

2.1.4 Shut-off mechanisms of active phosphodiesterase

Inactivation of E* is realized through GTP hydrolysis in the activated $G_{T\alpha\text{-}GTP}$-E* complex. The rate of this hydrolysis reaction is known to be modulated by three different players that all act through GTPase accelerating factors (GAFs): (1) the membrane associated protein complex RGS9 (He *et al.*, 1998), (2) the inhibitory subunits of PDE (PDE_γ, Arshavsky & Bownds, 1992; Tsang *et al.*, 1998), and (3) the non-catalytic cGMP binding sites in the α- and β-subunits of PDE (Yamazaki *et al.*, 1980; Cote *et al.*, 1994). The RGS9 complex is thought to be the most powerful of these. If one player of the RGS9 complex, RGS9-1, is knocked out, the rod photoresponse kinetics becomes significantly slower (Chen *et al.*, 2000). Also, if the RGS9 complex is overexpressed in mouse, their rods show an accelerated photoresponse kinetics (Krispel *et al.*, 2006). In fact, the experimental data from RGS9 overexpressing mice strongly suggest that the rod photoresponse recovery is rate-limited by E* shut-off through the RGS9 complex (Krispel *et al.*, 2006). The contributions of the mechanisms (2) and (3) are less clear. However, it is known that the GTP hydrolysis rate can be increased by the addition of PDE_γ (Arshavsky & Bownds, 1992). The physiological role of the non-catalytic cGMP binding sites seems to be small at least for short-term light exposures (Calvert *et al.*, 1998). It is, however, possible that these high-affinity cGMP binding sites may contribute to some slow light-adaptation phenomena. None of these GTPase accelerating mechanisms is known to be modulated by Ca^{2+}, consistent with the earlier data from amphibians that showed no modulation of the E* lifetime by background light (Nikonov *et al.*, 2000). Yet, Woodruff and others have recently published data that indicate acceleration of E* shut-off by background light in mouse rods (Woodruff *et al.*, 2008). Some evidence also suggests that the incorporation of a Ca^{2+}-dependent modulation on E* inactivation resolves some key inconsistencies between experiments and simulation (Kuzmin *et al.*, 2004; Hamer *et al.*, 2005).

2.1.5 Modeling phototransduction

This section presents a mathematical model that was used in this work to simulate dim flash responses measured with *ex vivo* ERG technique in normal and in very low $[Ca^{2+}]_o$. The goal was to find a model with maximal simplicity that still could explain the mouse rod flash photoresponses, i.e. the impulse response of the system and especially, its dependence on $[Ca^{2+}]_i$. The derivation largely follows that by Lamb and Pugh (Lamb & Pugh, Jr., 1992) and Nikonov and others (Nikonov *et al.*, 1998; Nikonov *et al.*, 2000). However, their approximations, based on low (< ~5 μM) physiological [cGMP], that assume a linear relation between the rate of cGMP hydrolysis and [cGMP] (Eq. (5)) and a direct proportionality of J_{cG} to $[cGMP]^{ncG}$ (Eq. (3)) were treated separately. Equations that allow simulation of impulse responses also in high [cGMP] are presented (Eqs. (2) and (11)). In the model it is assumed that ROS behaves as a well-stirred

volume with homogenous concentrations of cGMP and Ca^{2+}, i.e. their diffusion in the cytosol is expected to be fast compared to photoresponse kinetics. This approach has been successfully used in many modeling studies (see e.g. Nikonov *et al.*, 2000; Hamer *et al.*, 2003). A more detailed spatio-temporal model is also developed (Caruso *et al.*, 2005), but it would not provide significant additional value to this study. Instead, it would definitely increase the complexity of analysis and add some parameters whose values are not known with a reasonable precision. Since the rate of 2D diffusion of the phototransduction molecules in the disc membranes is not known to depend on $[Ca^{2+}]_i$, a constant value for the rate of E* production by single R* (= ν_E) is adopted as earlier done by Lamb and others (Lamb & Pugh, Jr., 1992, see also Lamb, 1994).

The output of the phototransduction system is the membrane current of ROS which consists of the CNG channel current (J_{cG}) and the exchanger current (J_{ex}). J_{cG} is a function of free cyclic GMP concentration ([*cGMP*]) in ROS and can be described by a Hill equation

$$J_{cG} = J_{cG,\max}\frac{[cGMP]^{n_{cG}}}{[cGMP]^{n_{cG}} + K_{cG}^{n_{cG}}}, \tag{2}$$

where $J_{cG,max}$ is the maximal CNG channel current at high [cGMP], K_{cG} is [cGMP] at which J_{cG}= ½$J_{cG,max}$, and n_{cG} is the cooperativity of the channel for cGMP. The K_{cG} is ~20 μM (reviewed in Pugh, Jr. & Lamb, 2000), which is much larger than the physiological value of [cGMP] (< 4 μM, reviewed in Lamb & Pugh, Jr., 1992) at any lighting condition. Thus, typically J_{cG} is approximated as

$$J_{cG} \approx \frac{J_{cG,\max}}{K_{cG}^{n_{cG}}}[cGMP]^{n_{cG}} \tag{3}$$

However, in a dark-adapted rod exposed to low Ca^{2+}, the [cGMP] might be close to or larger than K_{cG} and in that case Eq. (2) has to be used. $J_{cG,max}$ can be taken from experimental data (not available for mouse) or it can be inferred from the steady state values of J_{cG} and [*cGMP*] e.g. in darkness. However, some uncertainty is involved in the value of [*cGMP*] in darkness, which also is unavailable for mouse rod.

The NCKX1 current follows a Michaelis type equation with respect to $[Ca^{2+}]_i$ (Cervetto *et al.*, 1989; Hamer *et al.*, 2003)

$$\begin{cases} J_{ex} = J_{ex,\max}\dfrac{\left([Ca^{2+}]_i - [Ca^{2+}]_{\min}\right)}{\left([Ca^{2+}]_i - [Ca^{2+}]_{\min}\right) + K_{ex}} \approx \dfrac{J_{ex,\max}}{K_{ex}}\left([Ca^{2+}]_i - [Ca^{2+}]_{\min}\right), [Ca^{2+}]_i \geq [Ca^{2+}]_{\min} \\ J_{ex} = 0, \quad [Ca^{2+}]_i < [Ca^{2+}]_{\min} \end{cases}, \tag{4}$$

where $J_{ex,max}$ is the maximal exchanger current at high $[Ca^{2+}]_i$, $[Ca^{2+}]_{min}$ is the minimum intracellular calcium concentration that can be attained in bright light, and K_{ex} is $[Ca^{2+}]_i$ at which J_{ex} = ½$J_{ex,max}$. The experimentally determined value for K_{ex} (~1.5 μM >> $[Ca^{2+}]_i$,

Cervetto *et al.*, 1989) justifies the linear approximation. The form of Eq. (4) holds under physiological conditions, and it ensures that the calculated exchanger current does not reverse even in bright light (~20 - 50 nM for the mouse ROS). $J_{ex,max}$ is ~20 pA in a salamander rod (Lagnado *et al.*, 1992), and ~1-2 pA in the small mammalian rod (Schnetkamp, 1991). It can be also determined from the steady-state values of $[Ca^{2+}]_i$ and J_{ex} e.g. in darkness. $J_{ex,dark}$ can be determined from suction electrode responses to bright flashes or it can be inferred from the steady-state condition $d[Ca^{2+}]_i/dt = 0$ (see Eq. (12) below).

Next the equations for the time-dependent variable [*cGMP*] that determines the output of the system ($J_{cG} + J_{ex}$) will be deduced. In a well-stirred system the rate equation for the [*cGMP*] is often expressed as

$$\frac{d[cGMP]}{dt} \approx \alpha(t) - \beta(t)[cGMP], \tag{5}$$

where $\alpha(t)$ is the rate of cGMP synthesis from GTP by GCs (in μMs^{-1}, the expression assumes that [GTP] >> Michaelis constant of the synthesis reaction) and $\beta(t)$ is the hydrolysis rate of cGMP by all the PDE molecules in the ROS (in s^{-1}). The Eq. (5) assumes also that [cGMP] is much smaller than K_m of the cGMP hydrolysis reaction (assumption that cannot be made under very low $[Ca^{2+}]_o$, see below). The parameter β includes both the intrinsic hydrolytic activity of the PDE molecules in darkness (β_{dark}) and the light-induced activity of E*s

$$\beta(t) = \beta_{dark} + E^*(t)\beta_{sub}, \tag{6}$$

where β_{sub} is the rate of cGMP hydrolysis by a single activated PDE subunit (in s^{-1}) and E^* is given by Eq. (1). The rate of cGMP synthesis is a function of $[Ca^{2+}]_i$, and is expressed here as (Pugh, Jr. & Lamb, 2000)

$$\alpha(t) = \alpha_{\min} + \frac{\alpha_{\max} - \alpha_{\min}}{1 + \left(\frac{[Ca^{2+}]_i}{K_{cyc}} \right)^{m_{cyc}}}, \tag{7}$$

where α_{min} is the lowest GC activity at high $[Ca^{2+}]_i$ and α_{max} is the maximal activity at very low $[Ca^{2+}]_i$, K_{cyc} (~100 – 200 nM) is the half-activation concentration of $[Ca^{2+}]_i$ and m_{cyc} (2-3) is the Hill constant of the synthesis reaction (see Pugh, Jr. *et al.*, 1997). α_{min} is often approximated to be zero (Pugh, Jr. & Lamb, 2000). The experimental data on the α_{max} is scarce and not available for mouse. Alternatively, α_{max} can be estimated from the steady-state condition ($d[cGMP]/dt|_{t=0} = 0$) in darkness, which requires information about $[cGMP]_{dark}$ and β_{dark}.

At early times after a short light stimulus the Eq. (1) becomes (Lamb & Pugh, Jr., 1992; Nikonov *et al.*, 1998)

$$E^*(t) = \Phi \nu_E t\,. \tag{8}$$

At sufficiently early times, when the deactivation reactions can be omitted and α has had no time to change and can be treated as a constant, the differential Eq. (5) can be solved with the initial value $[cGMP](t = 0) = [\mathrm{cGMP}]_0$ to give

$$[cGMP] = [\mathrm{cGMP}]_0 \exp\left[-\tfrac{1}{2}\Phi \nu_E \beta_{sub} t^2\right]. \tag{9}$$

Substituting this to Eq. (3) yields

$$J_{cG}(t) = J_{cG}(0)\exp\left[-\tfrac{1}{2}\Phi \nu_E \beta_{sub} n_{cG} t^2\right] = J_{cG}(0)\exp\left[-\tfrac{1}{2}\Phi A t^2\right] \tag{10}$$

where $J_{cG}(0)$ is the initial steady-state CNG channel current before the impulse stimulus and A is an amplification constant that describes the gain of the activation reactions (in s^{-2}, Lamb & Pugh, Jr., 1992). Eq. (10) has been shown to properly describe the early rising phase of photoresponses in physiological conditions. However, the whole derivation was based on the assumption that [cGMP] is much smaller than the Michaelis constant of cGMP hydrolysis reaction by PDE (= K_m). In the very low Ca^{2+} conditions used in papers II and III this assumption is not valid anymore and we need to rephrase Eq. (5)

$$\frac{d[cGMP]}{dt} = \alpha(t) - \beta(t) K_m \frac{[cGMP]}{[cGMP] + K_m}, \tag{11}$$

which converges to Eq. (5) when [cGMP] << K_m. The current estimate for K_m is as small as 10μM (Leskov *et al.*, 2000), illustrating the necessity for using Eq. (11) if [cGMP] increases from the physiological value (~4 μM). A similar equation in slightly different form has been introduced earlier by Kuzmin and others (Kuzmin *et al.*, 2004). This equation was used in numerical calculations of flash responses in very low $[Ca^{2+}]_o$ (paper III).

To be able to simulate the full time course of flash responses the time-behavior of $[Ca^{2+}]_i$ has to be calculated, since both the GC activity and R* lifetime are strongly dependent on $[Ca^{2+}]_i$. Assuming a rapidly equilibrating Ca^{2+} buffer (buffering capacity B_{Ca}) the rate of $[Ca^{2+}]_i$ change is determined by Ca^{2+} influx through the CNG channels and extrusion by the NCKXs as

$$\frac{d[Ca^{2+}]_i}{dt} = -\frac{\tfrac{1}{2} f_{Ca} J_{cG}(t) - J_{ex}(t)}{F V_{cyto} B_{Ca}}, \tag{12}$$

where f_{Ca} is the fraction of the CNG channel current carried by Ca^{2+} (10 – 15%), F is Faraday's constant describing the charge carried by one mole of monovalent cations, and V_{cyto} is the cytoplasmic volume of ROS. The factor ½ takes into account that single Ca^{2+} molecule carries two elementary charges while factor is unity for the outflow because the extrusion of one Ca^{2+} yields to a net inflow of one elementary charge. It has been shown that the equations presented so

far allow the simulation of the full time course of mouse rod dim flash responses quite accurately (Nikonov *et al.*, 1998). However, a full model including a Ca^{2+} dependent modulation of R* lifetime is required to accurately describe the recovery kinetics of rod responses to brighter flashes. One way to include the modulation of τ_R is to assume that it is inversely proportional to the free concentration of RK ($[RK]_{free}$). There, free RK refers to those RK molecules that are not bound to recoverin. $[RK]_{free}$ in turn depends on the $[Ca^{2+}]_i$ in the ROS. A biochemical scheme with first order chemical reactions between RK, Ca^{2+}-bound recoverin and Ca^{2+} -free recoverin as well as reactions between Ca^{2+} and recoverin enables simulation of $[RK]_{free}$, and has been implemented e.g. by Nikonov *et al.* (Nikonov *et al.*, 2000) and Hamer *et al.* (Hamer *et al.*, 2005) to give a good description of rod responses to dim and bright light flashes.

2.2 Physical and chemical properties of Ca^{2+} signaling proteins in ROS

2.2.1 Physical and chemical properties of Ca^{2+} and other cations

In rod photoreceptor cells the most abundant cations are Na^+ (~10^{-2} M) , K^+ (~ 10^{-1} M), Mg^{2+} (free concentration ~ 10^{-3} M) and Ca^{2+} (free concentration ~10^{-7} - 10^{-8} M). The 10^7 – 10^4 –fold excess of the other cations compared to Ca^{2+} indicates that to function effectively the Ca^{2+} signaling proteins require that these proteins bind Ca^{2+} with much higher affinity compared to other prevalent cations, i.e. the specificity of the Ca^{2+} binding sites ought to be very high. It has been shown that the monovalent cations (Na^+ and K^+) can be discriminated effectively. This is thought to arise from the fact that a single charge cannot stabilize the repulsion between the coordinating ligands of the Ca^{2+} binding site (Falke *et al.*, 1991). The selectivity over Mg^{2+} which is chemically very similar to Ca^{2+} is less obvious and will be discussed shortly here and in the chapter 2.2.3.

All physiologically important cations mentioned above (Na^+, K^+, Mg^{2+}, Ca^{2+}) belong to the group of spherical metal ions. The outermost electronic shell of these ions is filled and their interaction with ligands is dominated by ionic forces instead of covalent binding, i.e. they are considered as “hard” metal ions. Consequently, the ligands that coordinate mostly through ionic interactions (e.g. oxygen) are preferred by spherical cations. The coordination chemistry of spherical ions is simply determined by their willingness to maximize the amount of coordinating ligands around the cation. The number of coordinating ligands (coordination number = CN) is thus related to the ionic radius (r_i). For Ca^{2+} (r_i = 1.00 Å) the usual CN in Ca^{2+} binding site is 7 whereas smaller Mg^{2+} (r_i = 0.72 Å) prefers 6 coordinating ligands.

In an aqueous solution cations are hydrated, i.e. they are coordinated by water molecules. The hydration energy increases as a function of surface charge density, for divalent cations it is roughly inversely proportional to the ionic radius. Hence, the energetic cost of dehydration that must happen upon binding is larger for Mg^{2+} than for Ca^{2+}. This probably contributes to the higher affinity of Ca^{2+} compared to Mg^{2+}. The water substitution rate is quite fast for Ca^{2+} (~10^8

s^{-1}) indicating that Ca^{2+} binding might be diffusion limited in many cases (Falke *et al.*, 1994), however, for Mg^{2+}, with water substitution rate of ~10^5 s^{-1}, the dehydration process might contribute to the binding kinetics.

Transition metals include groups 4-11 (sometimes also group 12 is included) in the periodic table of elements. They are defined as atoms that have an incomplete d sub-shell. Many transition metals, like those of period 4 (the first row transition metals), form divalent cations in aqueous solution. Physiologically relevant transition metal cations from period 4 include manganese (Mn^{2+}), iron (Fe^{2+}), cobalt (Co^{2+}), copper (Cu^{2+}) and zinc (Zn^{2+}). However, the total concentration of these elements in cells is much lower compared to Ca^{2+} and Mg^{2+}, and moreover, transition metals are mostly bound to their target molecules. Cobalt, which donates two electrons from the outermost 4s sub-shell in water to make divalent cation Co^{2+}, whose outermost d sub-shell have 7 electrons (3 unpaired electrons). The ionic radius of Co^{2+} is ~0.7 Å, very similar to that of Mg^{2+}. As expected, also its water substitution rate and hydration energy is similar to that of Mg^{2+}. Transition metal cations are softer compared to spherical metals showing more tendency to covalentic binding, and prefer softer (= more polarizable) nitrogen and sulfur ligands. Due to unpaired electrons, transition metals, including cobalt, are paramagnetic.

2.2.2 CNG channel and NCKX which control the $[Ca^{2+}]_i$

The functional properties of the CNG channels and NCKXs have been extensively studied while the 3D structure and thus the detailed molecular mechanisms of e.g. the ion selectivity of these two integral membrane proteins remain largely unknown.

The vertebrate rod CNG channel is a heterotetramer composed of 3 CNGA1 and one CNGB1 subunit (Zhong *et al.*, 2002). The relative permeabilities (P) of different alkaline mono- and divalent cations as well as some organic cations have been investigated by suction electrode recordings (Yau *et al.*, 1981) or from the outer segment membrane patches (Fesenko *et al.*, 1985). The results indicate that the channel can permeate alkaline monovalent cations with a permeability sequence Na^+ ~ lithium (Li^+) > K^+ > rubidium (Rb^+) > Cs^+ (for review see discussion in Furman & Tanaka, 1990). It can also pass the organic cation guanidium$^+$ (Nakatani & Yau, 1988b) but not choline$^+$, TEA$^+$ or tetramethylammonium$^+$ (Hodgkin *et al.*, 1985). The divalent cations Ca^{2+} Sr^{2+}, Ba^{2+}, Mg^{2+} and Mn^{2+} can permeate the CNG channel but they also show complex voltage-dependent blocking effects, probably through entering the channel and decreasing its conductance (Menini *et al.*, 1988). From the extensive data about the CNG channels, attempts have been made to understand the selectivity mechanism of the channel. A simple electrostatic model can be used to explain the selectivity by considering the energies related to the dehydration energy and the attractive electrostatic energy of the binding site (see Eisenman & Horn, 1983). The model predicts different permeability sequences with different field strengths of the binding site. The results from the rod CNG channel indicate very high field strength of the cation binding site (Picco & Menini, 1993). Addition-

ally, one can try to estimate the size of the narrowest place in the channel pore by finding the largest cation that can permeate the channel. This kind of comparison yields to approximation of a rectangular pore with dimensions of 0.38 x 0.5 nm (Picco & Menini, 1993).

In mammalian ROS Ca^{2+} is continuously extruded by a plasma membrane exchanger that is coded by the NCKX1 gene (Reilander *et al.*, 1992). The secondary structure of NCKX consists of 10 transmembrane and one cytosolic helix connecting the 5th and 6th helix (Kinjo *et al.*, 2003). It is thought that the extrusion of Ca^{2+} is achieved by large conformational changes in the exchanger protein (see Altimimi & Schnetkamp, 2007). Direct structural data to support this is, however, still lacking. The NCKXs seem to be very specific in regards to Na^+, and not even the very widely used substitute Li^+ can drive extrusion of Ca^{2+} (Yau & Nakatani, 1984). K^+ in the Ca^{2+} extrusion cycle can be replaced by Rb^+ and ammonium ion (NH_4^+) but not by Na^+ or Li^+ (Schnetkamp & Szerencsei, 1991; Prinsen *et al.*, 2002). NCKXs can extrude Sr^{2+} but neither the common divalent cations Mg^{2+}, Mn^{2+} or Ba^{2+} nor trivalent cations (Schnetkamp, 1980; Yau & Nakatani, 1984; Schnetkamp, 1991). Instead, they compete with Ca^{2+} in the NCKX's Ca^{2+} binding site and thereby block the action of the exchanger.

2.2.3 GCAP and recoverin are EF-hand proteins that mediate Ca^{2+} signal in the rod outer segment

Ca^{2+} signals are mediated by specialized Ca^{2+} sensor proteins. The largest group is the EF-hand superfamily to which also GCAP and recoverin belong. They use a conserved helix-loop-helix structure (EF-hand = EFh) to bind Ca^{2+} (see Figure 2A). The EFh motif contains 29 amino acids that form the E and F helices linked by a loop of 12 residues of which 6 (1st, 3rd, 5th, 7th, 9th and 12th residue of the loop) participate to Ca^{2+} coordination with their side chain or backbone carboxylate group ($-COO^-$). The 12th amino acid (usually glutamate) can form two coordinating "bonds" (bidendate coordination) so that the CN for Ca^{2+} is 7 in the EF-hand Ca^{2+} binding sites. Five of the coordinating oxygen atoms in the EFh binding pocket form approximately a planar pentagonal array and two lie axial to this plane, constituting a bipyramidal pentagonal coordination geometry (Figure 2B). The 9th residue typically provides an indirect coordination through a water molecule. The lower affinity of Mg^{2+} to the EF-hand binding site is thought to arise from the larger dehydration energy of Mg^{2+} due to its smaller ionic radius and its preference for an octahedral coordination geometry. When Mg^{2+} is bound to the EFh binding site, the 12th coordinating amino acid provides only monodendate coordination leading to a different overall conformation of the EFh protein (which often is not functional) compared to the Ca^{2+} -bound molecule (see e.g. Ozawa *et al.*, 2000). The EF-hand protein family is diverse and it contains Ca^{2+} binding proteins with versatile functions and different affinities to Ca^{2+}. The EFh motifs form almost always pairs, and thus the EFh proteins typically have an even number (2, 4 or 6) of Ca^{2+} binding sites. Binding to these sites is usually strongly co-operative enabling sharp responses to small changes of $[Ca^{2+}]_i$.

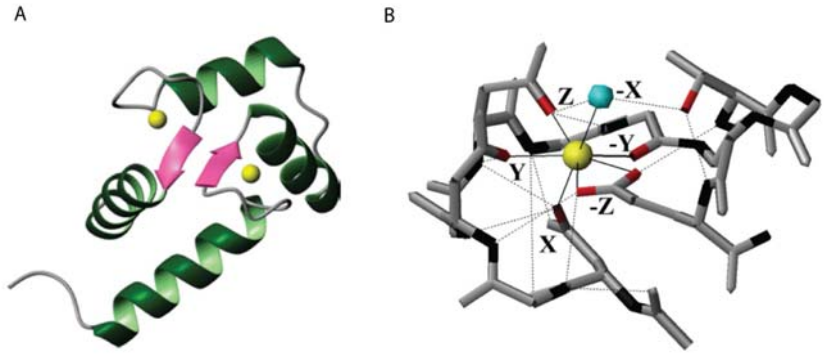

Figure 2 Structure of the EF-hand. (A) A pair of EF-hands with bound Ca^{2+} (yellow). This Figure was originally published in Gifford *et al.* (2007), © the Biochemical Society. (B) Pentagonal pipyramidal coordination geometry of the EF-hand Ca^{2+} binding site. This Figure was originally published in Gifford *et al.* (2007), © the Biochemical Society.

Recoverin and GCAP belong to the family of neuronal calcium sensor (NCS) proteins. They both include four EFh motifs of which EF-1 cannot bind Ca^{2+} (Flaherty *et al.*, 1993; Ames *et al.*, 1999). In recoverin also EF-4 is unable to bind Ca^{2+} (Flaherty *et al.*, 1993). Recoverin contains a hydrophobic fatty acyl "tail" called myriostyl group that is buried into the Ca^{2+} -free recoverin but exposed to solvent upon Ca^{2+} binding (Tanaka *et al.*, 1995). The 3D structures of recoverin and GCAP are very similar, and their two EFh pairs form a compact tandem array contrasting the dumbbell shape of the other well-studied EF-hand protein, calmodulin.

The structure and function of recoverin has been studied extensively. The 3D structures for myriostylated recoverin with 0, 1 and 2 bound Ca^{2+} as well as for the myriostylated rec-2Ca^{2+}-rhodopsin kinase complex bound have been determined (Tanaka *et al.*, 1995; Ames *et al.*, 1997; Ames *et al.*, 2002; Ames *et al.*, 2006). These studies have suggested a sophisticated molecular mechanism for recoverin that modulates the R* lifetime (Ames *et al.*, 2006). In darkness recoverin has bound two Ca^{2+} and the extruded myriostyl group favors the binding of recoverin to membranes. Further, the Ca^{2+} -bound recoverin has adopted an open conformation with a specific hydrophobic region exposed to solvent and that can bind to rhodopsin kinase. In this way recoverin can sterically prevent RK from phosphorylating R*. When light decreases $[Ca^{2+}]_i$, Ca^{2+} is relieved from the Ca^{2+} binding sites of recoverin. Subsequently, recoverin adopts a closed conformation and sequesters the myriostyl group. This conformation change detaches recoverin from RK and the disc membrane, enabling RK to phosphorylate R* and thereby decrease its lifetime. However, in spite of the detailed structural and mechanistic knowledge on recoverin function, some inconsistencies regarding to the physiological role of recoverin still remain. Firstly, the biochemically measured affinity ($K_D \approx 3$ μM, Chen *et al.*, 1995a; Klenchin *et al.*, 1995) of the myriostylated recoverin to Ca^{2+} does not match the range of free $[Ca^{2+}]_i$ in ROS. Secondly, R* phosphorylation has been shown to be

independent of [Ca^{+}] in the α-toxin permeabilized rods (Otto-Bruc *et al.*, 1998).

The structure of unmyriostylated GCAP-2 (Ames *et al.*, 1999) and myriostylated GCAP-1 (Stephen *et al.*, 2007) with 3 Ca^{2+} bound have been determined. Thus far the Ca^{2+} -free conformation of GCAP has not been determined, and the molecular mechanism of GCAP action remains to be discovered. It is known that the Ca^{2+} bound GCAP cannot activate membrane bound retGC and might inhibit it. As light decreases $[Ca^{2+}]_i$, Mg^{2+} replaces Ca^{2+} in the EFh binding sites of GCAP, and it is the Mg^{2+} bound GCAP that can activate GC (Peshenko & Dizhoor, 2007; Dizhoor *et al.*, 2010). The macroscopic dissociation constant of Ca^{2+} determined *in vitro* at 1 mM [Mg^{2+}] is ~100 nM, matching well to the physiological range of $[Ca^{2+}]_i$ in ROS.

2.3 Ionic mechanisms in the rod inner segment; generation of the rod V_m signal

The steady state value of V_m as well as its dynamics in response to light stimulus are strongly influenced not only by the outer segment mechanisms, but also by the ionic mechanisms of the rod inner segment and synaptic region plasma membrane (e.g. Schwartz, 1981; Barnes, 1994). These mechanisms also contribute to the extracellular voltage measured across the photoreceptor layer or across the whole retina by forming current dipoles between unevenly distributed current sinks and sources in the photoreceptor plasma membrane along the rod (paper I).

Simultaneous recordings of the outer segment current ($J_{cG} + J_{ex}$) and membrane voltage from the large salamander rod photoreceptors have indicated that in response to a light flash the ROS current and V_m initially follow the same kinetics, but the recovery of V_m is accelerated compared to the current response (see Figure 3B,C). Additionally, in response to bright flashes V_m shows a transient negative peak which relaxes to a plateau level. Intracellular and patch clamp recordings from amphibian and mammalian rods have shown that the membrane potential is near -40 mV in darkness and relaxes after the initial negative peak to a steady state value between -50 and -60 mV as a response to bright light (Figure 3C-E).

Although the inner segment conductance mechanisms have not been studied as extensively as the CNG channel current, the main ionic mechanisms have been characterized at least in amphibian rods. The studies of the ionic mechanisms of the mammalian RIS are, however, much more sparse. Some data is available for guinea-pig (Demontis *et al.*, 1999), porcine (Cia *et al.*, 2005), rabbit (Demontis *et al.*, 2002), primate (Schneeweis & Schnapf, 1995) and human (Kawai *et al.*, 2001). Notably, only a very few voltage recordings from mouse rods are available (Okawa *et al.*, 2008; Demontis *et al.*, 2009), and information on channel properties at 37°C is even more limited. Figure 3A shows the physiologically relevant conductance mechanisms found in the vertebrate rod plasma membrane. The rod inner segment contains the Na^{+}-K^{+} ATPases that maintain the potassium (K^{+}) and sodium ion gradients across the cell membrane by extruding K^{+}

and intruding Na^+ with energy provided by ATP hydrolysis (e.g. Hagins *et al.*, 1975; Schneider *et al.*, 1991). Unlike in the outer segment, the extrusion of Ca^{2+} in RIS is mainly realized by Ca^{2+} ATPases (PMCAs, Krizaj & Copenhagen, 1998). The rod inner segment plasma membrane includes also many voltage- and/or Ca^{2+} -gated ion channels that carry Na^+, K^+, Ca^{2+} and Cl^- currents. The properties of the channels, treated in the following sections, are summarized in Table 1.

2.3.1 Hyperpolarization activated cation channel (HCN1)

The inner segments of vertebrate rods contain channels that are closed in darkness ($V_m \approx$ -40 mV) and are opened by membrane hyperpolarization (Fain *et al.*, 1978; Attwell & Wilson, 1980; Bader *et al.*, 1982). The current, I_h, is carried by Na^+ and K^+, and its reversal potential E_h is ~ -30 mV (Bader *et al.*, 1982; Hestrin, 1987). The h channels have been found also in many mammalian rods: guinea-pig (Demontis *et al.*, 1999), rabbit (Demontis *et al.*, 2002), porcine (Cia *et al.*, 2005), mouse (Knop *et al.*, 2008) and human (Kawai *et al.*, 2002). The rod photoreceptor h channels seems to be comprised of HCN1 isoform (Demontis *et al.*, 2002; Knop *et al.*, 2008). The HCN1 channels are found along the whole inner segment (including cell body, axon and synaptic terminal, Demontis *et al.*, 2002; Knop *et al.*, 2008). However, the channel density along the inner segment is not known.

The physiological importance of HCN1 channels in modulating the voltage response of rod photoreceptors to bright light stimulus have been indicated in many studies. I_h limits the hyperpolarization of V_m, which may help to prevent the saturation of the synaptic L-type Ca^{2+} channels (see Leeper & Copenhagen, 1979; Attwell *et al.*, 1987; Barnes, 1994 and 2.3.3). Another important effect of h channels is to accelerate the photoresponse recovery, and thus to improve the temporal resolution of rod-based vision (Demontis *et al.*, 1999; Gargini *et al.*, 1999). However, the leading edge of voltage responses to bright flashes is probably not affected by the h channels, because their gating is rather slow (see below). This is also consistent with the mutual initial time course of rod's current and V_m photoresponse (see Figure 3B-C, Baylor *et al.*, 1984).

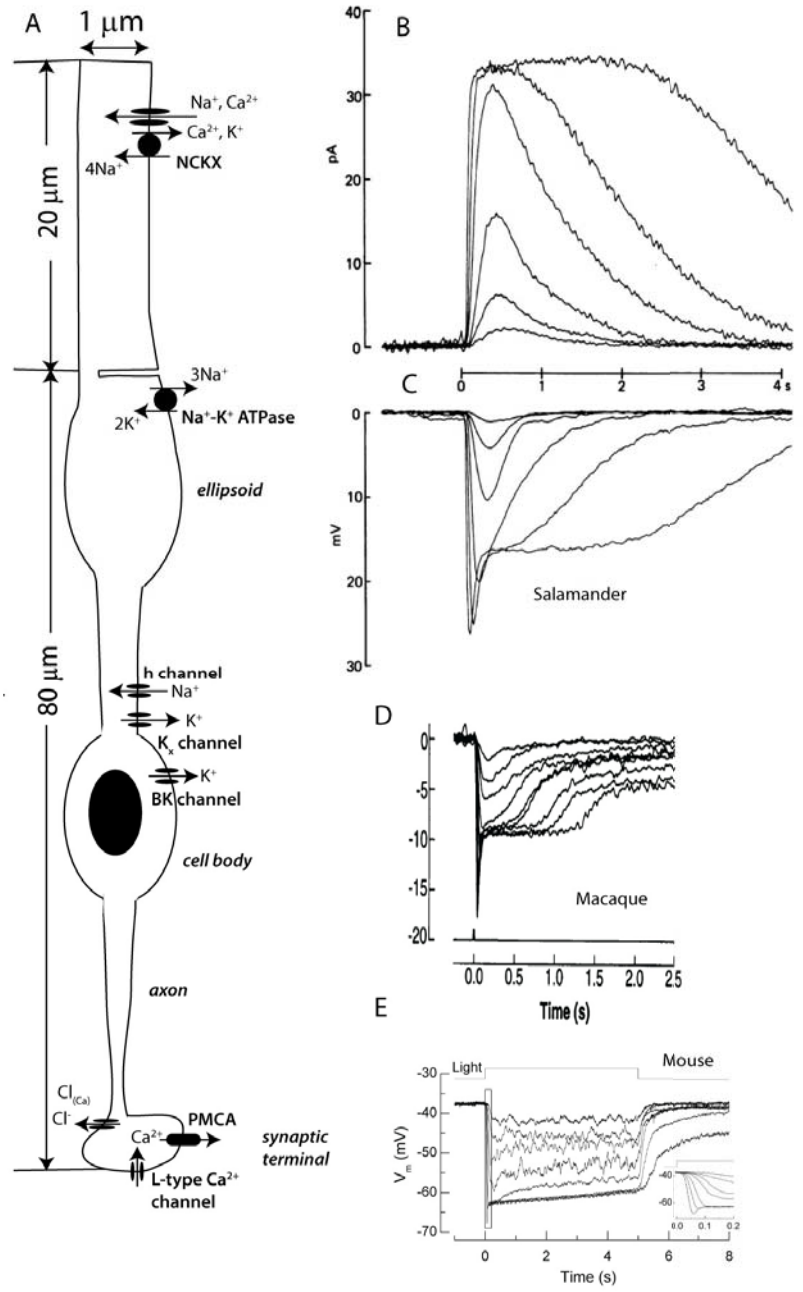

Figure 3 (A) Ionic mechanisms of the rod plasma membrane. (B) Current photoresponses of a salamander rod outer segment. Reprinted with permission from Baylor *et al.* (1984), © Wiley-Blackwell Ltd. (C) Simultaneous V_m flash photoresponses of the same salamander rod and to identical stimuli as in A. Reprinted with permission from Baylor *et al.* (1984), © Wiley-Blackwell Ltd. (D) V_m flash photoresponses from a macaque rod. Reprinted with permission from Schneeweis & Schnapf (1995), © American Association for the Advancement of Science. (E) V_m photoresponses to 5 second steps of light as recorded from a mouse rod. Reprinted with permission from Okawa *et al.* (2008), © Elsevier Ltd.

Table 1 Properties of rod inner segment voltage gated channels. Numerical data is almost exclusively obtained from salamander rods at room temperature. E_r = reversal potential, τ = time constant of channel activation, I_{dark} = channel current in darkness ($V_m \approx$ -40 mV), ΔI_{light} = effective direction of light (hyperpolarization) induced current response. More details in the text.

Channel	Permeability	E_r (mV)	Gating range (mV)	τ (ms)	I_{dark} (pA)	ΔI_{light}	Blockers
h	Na^+, K^+	-30	< -50	50 – 250	0	Inward	Cs^+, ULFS49, S16257
Kx	K^+	-75	> -60	25 – 250	+40	Inward	Ba^{2+}, TEA
BK	K^+	-75	-30…+40	~100	+10	Inward	IbTx, ChTx, TEA
Ca_v	Ca^{2+}	+50	-40…+50	< 20	Negative	Outward	Cd^{2+}, Co^{2+}, verapamil, diltiazem
Cl(Ca)	Cl^-	0…-20	-40…+60	~100	Negative	Outward	NifA, NPPB

The studies by intracellular and patch clamp recordings have indicated that the initial transient peak of V_m response to bright light (see Figure 3C-F) is generated by the h channels (Fain *et al.*, 1978; Capovilla *et al.*, 1981). Bright light induces a sufficient hyperpolarization that opens the h channels and an inward cationic current (negative I_h because $V_m < E_h$) causes a repolarization of V_m (and consequent decrease of $|I_h|$) to a plateau level. The h channels can be pharmacologically blocked by extracellularly applied Cs^+ (in mM range) which also removes the peak-plateau behavior and lets V_m to hyperpolarize close to E_K (~ -75 mV) in bright light (Fain *et al.*, 1978). Organic compounds zatebradine and ivabradine are known to inhibit I_h. Additionally, protons and Ca^{2+} modulate the voltage-dependency of the rod h channels (Malcolm *et al.*, 2003). Actually, it was shown already in 1977 that the peak-plateau process disappears in very low $[Ca^{2+}]_o$ (< 50 nM, Lipton *et al.*, 1977).

The h channels start to open at V_m of *ca.* -50 mV and the maximal conductance is achieved at ~ -90 mV ($G_{max} \approx$ 1-2 nS, Hestrin, 1987; Demontis *et al.*, 2002; Kawai *et al.*, 2002). A full Hodgkin-Huxley-based model (HH model, Hodgkin & Huxley, 1952), that would accurately describe the kinetics of the h channel gating is not available (see Hestrin, 1987). Yet, the h channel behavior has been approximated with single activation gate (n_h) in the context of modeling the rod's V_m response (Kourennyi *et al.*, 2002; Liu & Kourennyi, 2004a). The h channel opening is slow and voltage-dependent. The activation time constant (τ_h) of the channels is ~50 – 250 ms when V_m is clamped to ~-100 - -50 mV from the holding potential of -30 - -40 mV (Hestrin, 1987; Demontis *et al.*, 1999; Demontis *et al.*, 2002; Demontis *et al.*, 2009).

2.3.2 Depolarization- and Ca^{2+}- activated K^+ channels (Kx, BK)

In darkness, the inflow of cations through the ROS CNG channels is largely balanced by the outflow of K^+ through voltage- and/or Ca^{2+} -gated channels. The outward current seems to be distributed along the whole inner segment and is absent from the outer segment (Penn & Hagins, 1969; Hagins *et al.*, 1970). Rod photoreceptors contain at least two types of K^+ channels: Kx and BK channels. The voltage-

dependent Kx channels and the Ca^{2+}-activated BK channels contribute in setting the membrane potential in darkness (Beech & Barnes, 1989; Moriondo *et al.*, 2001). The Kx current is also known to accelerate the V_m response recovery after a light flash or a hyperpolarizing current pulse and to contribute to high pass filtering properties of the rod photoreceptors (Owen & Torre, 1983; Demontis *et al.*, 1999). The K^+ channel densities in different regions of the rod plasma membrane as well as their molecular composition are still unclear. However, recent results suggest that the Kx channels in mammalians might be composed of Kir2.4 channel proteins (Hughes *et al.*, 2000; Cheng *et al.*, 2006; Demontis *et al.*, 2009).

The voltage-dependency and kinetics of the Kx current resemble to those of the M current found in many neurons. The macroscopic conductance G_{Kx} reaches maximal value at ca. -30 mV (~1 nS in salamander rods) and the channels are closed when V_m is below -60 mV (Beech & Barnes, 1989). The reversal potential is the same as K^+ equilibrium potential E_K = -75 mV (Beech & Barnes, 1989). The deactivation and activation kinetics can well be described by single exponential time constants (τ_{Kx}) that are voltage-dependent. The HH model with a single activation gate yields a good description of $\tau_{Kx}(V_m)$. The τ_{Kx} is largest at around the dark resting V_m (~250 ms) and declines to ca. 25 ms at -100 mV in salamander rods (Beech & Barnes, 1989). Similar gating and kinetic properties describe also mammalian I_{Kx} well (Demontis *et al.*, 1999). The Kx channels, like other K^+ channels, can be inhibited by TEA (10 – 30 mM) or intracellularly applied Cs^+ (Attwell & Wilson, 1980; Bader *et al.*, 1982; Beech & Barnes, 1989; Demontis *et al.*, 1999; Liu & Kourennyi, 2004a). Barium (Ba^{2+}) affects strongly the gating of the Kx channels, e.g. 5 mM $[Ba^{2+}]_o$ moves the activation range of the Kx channels of salamander rods to 40 mV more positive V_m values (Beech & Barnes, 1989). The M-current is suppressed by several neurotransmitters, but currently such effects on the Kx channels have not been found. As with many other voltage-gated channels, protons modulate I_{Kx} (Kurenny & Barnes, 1994).

The most relevant Ca^{2+} -activated K^+ channel in photoreceptors seems to be the large conductance BK channel, although also the intermediate conductance IK channels are expressed in salamander rods (Pelucchi *et al.*, 2008). Xu and Slaughter (Xu & Slaughter, 2005) localized the BK channels almost exclusively to rod terminals, but a more recent study suggests that the BK channels are distributed along the whole inner segment with highest density at the ellipsoid region (Pelucchi *et al.*, 2008). The BK channels are thought to contribute in setting the membrane potential in darkness. They activate upon an increase in $[Ca^{2+}]_i$ and can thus oppose the depolarizing effect caused by the Ca^{2+} inflow through L-type Ca^{2+} channels. The BK channels are open between ca. -30 mV and +40 mV under physiological $[Ca^{2+}]_i$ homeostasis and their gating kinetics is very fast compared to the Kx channels (Moriondo *et al.*, 2001). I_{BK} can be indirectly suppressed by blocking the L-type Ca^{2+} channels (see below) or more specifically by charybdotoxin (ChTx, ~10^{-7} M) and iberiotoxin (IbTx, ~10^{-7} M) or by 1 mM [TEA]. Other BK channel inhibition strat-

egies include the use of intracellularly applied Ca^{2+} chelators (e.g. EGTA) or replacement of Ca^{2+} by Ba^{2+} which cannot activate I_{BK}.

2.3.3 Ca^{2+} homeostasis; role of L-type Ca^{2+} channels and Ca^{2+} ATPase

The release of glutamate at the rod ribbon synapse is controlled by $[Ca^{2+}]_i$ in the synaptic region (Rieke & Schwartz, 1996). At the rod synaptic terminal $[Ca^{2+}]_i$ is mainly determined by the inflow of Ca^{2+} through the voltage-gated Ca^{2+} channels (Schwartz, 1981; Bader *et al.*, 1982; Corey *et al.*, 1984; Schmitz & Witkovsky, 1997) and its extrusion by Ca^{2+} ATPase (PMCA, Krizaj & Copenhagen, 1998). Both the Ca^{2+} channels and PMCAs are found at the rod synaptic terminals and possibly along the whole inner segment (Krizaj & Copenhagen, 1998; Nachman-Clewner *et al.*, 1999; Cia *et al.*, 2005).

A voltage-gated Ca^{2+} current was described by Bader et al. (1982) (see also Schwartz, 1981) from salamander rods and further characterized by Corey et al. (Corey *et al.*, 1984). Recordings from salamander rods have shown that I_{Ca} starts to activate at *ca.* -40 mV, reach its peak near 0 mV, and deactivates at around +50 mV which is also presumably near the equilibrium potential E_{Ca} of Ca^{2+} (Bader *et al.*, 1982; Corey *et al.*, 1984; Rieke & Schwartz, 1994). It appears that the voltage-gated Ca^{2+} channels in rods are L-type channels and they activate and deactivate rapidly compared to the h or Kx channels (a steady-state is achieved in less than 20 ms after a V_m jump). They do not exhibit voltage-dependent inactivation but may show slow Ca^{2+} -dependent inactivation. The single Ca^{2+} channels of salamander rods have two closed states and a single open state with a single channel conductance $g_{Ca} \approx 20$ pS (Thoreson *et al.*, 2000). The L-type Ca^{2+} channels are pharmacologically defined from their sensitivity to dihydropyridines (antagonists: nifedipine and nitrendipine and agonist: Bay K 8644). They can carry Ba^{2+} and Sr^{2+} currents but are blocked by Cd^{2+} (~10^{-4} M) and Co^{2+} (~10^{-3} M). The L-type Ca^{2+} channels in rods can also be blocked by verapamil and diltiazem. Like most voltage-gated channels also L-type Ca^{2+} channels are sensitive to pH (Barnes *et al.*, 1993). Distinctively from other L-type Ca^{2+} channels, low intracellular chloride $[Cl^-]_i$ has been shown to decrease the single Ca^{2+} channel open probability in rods (Thoreson *et al.*, 2000).

Currents through $Ca_v1.4$ calcium channels in various expression systems (e.g. HEK293 cells) resembles the Ca^{2+} currents measured from intact cells, especially if the expression system is provided with the Ca^{2+} binding protein CaBP4 (Baumann *et al.*, 2004; Haeseleer *et al.*, 2004; Doering *et al.*, 2007). The $Ca_v1.4$ proteins have been immunolocalized at photoreceptor terminals, and the mouse carrying a mutation in $Ca_v1.4$ protein shows disruption of Ca^{2+} signaling at the synaptic terminal as well as serious problems with synaptic transmission from rods to second-order neurons (Mansergh *et al.*, 2005). These studies strongly imply that the L-type Ca^{2+} channels in rods are comprised of the $Ca_v1.4$ protein. However, the results from electrophysiological studies suggest that the conductance of Ca^{2+} channels is very small already in darkness and that I_{Ca} should decline to zero by only a few mV hyperpolarization. This would mean that the glutamatergic

synaptic transmission would saturate already at dim light. The synaptic signal transfer from rods to horizontal and bipolar cells actually has shown this kind of signal "clipping" in a salamander retina (Attwell, 1986; Attwell *et al.*, 1987). Alternatively, at least in salamander cones, other Ca^{2+} entry pathways might contribute to the synaptic Ca^{2+} homeostasis (Rieke & Schwartz, 1994; Savchenko *et al.*, 1997). It is also possible that the experimental conditions used to isolate L-type Ca^{2+} current in rods or in various expression systems shift the activation curve of the I_{Ca} towards more positive values (Doering *et al.*, 2007). Interestingly, the few studies of the L-type Ca^{2+} current in intact mammalian photoreceptors show activation at more negative V_m compared to those in amphibians (Yagi & MacLeish, 1994; Morgans *et al.*, 2005; Cia *et al.*, 2005), e.g. in porcine rods the I_{Ca} is activated already at ca. -60 mV (Cia *et al.*, 2005).

2.3.4 Ca^{2+} -activated chloride (Cl^-) current ($I_{Cl(Ca)}$)

An anionic chloride (Cl^-) conductance that is activated by Ca^{2+} was first found in the salamander rod inner segment (Bader *et al.*, 1982). Its reversal potential (i.e. equilibrium potential of E_{Cl}) seems to be between -10 and -20 mV, meaning that at physiological voltage range ($V_m < E_{Cl}$) $I_{Cl(Ca)}$ is always inward, i.e. Cl^- efflux is present when the channels are open (Thoreson *et al.*, 2000; Thoreson *et al.*, 2003). The Cl channel is not effectively opened by Ba^{2+} and it can be blocked with niflumic acid (NifA, 0.1 mM) or benzoic acid (NPPB, 2 μM). Alternatively, $I_{Cl(Ca)}$ can be inhibited by the L-type Ca^{2+} channel antagonists. $I_{Cl(Ca)}$ has also been characterized in mammalian rods where it is activated at V_m values positive to -60 mV and it reverses at around 0 mV (Yagi & MacLeish, 1994; Cia *et al.*, 2005). The Ca^{2+} -activated Cl^- efflux has been shown to inhibit the L-type Ca^{2+} current (Thoreson *et al.*, 2000). Thus, $I_{Cl(Ca)}$ may introduce a negative feedback control of Ca^{2+} influx, and consequently modulate synaptic transmission.

2.3.5 Modeling V_m responses

Although a full set of channel gating parameters, especially for mammalian rods, is not available, some attempts have been made to simulate the rod V_m response to light (Kourennyi *et al.*, 2002; Liu & Kourennyi, 2004a; Liu & Kourennyi, 2004b). These simulations assume an isopotential cell and use the channel parameters extracted from amphibian rods. The cell can be modeled as an electrical circuit with separate conductances in parallel. The total current across the rod plasma membrane can be written as

$$\begin{aligned} I_T = C\frac{dV_m}{dt} + J_{cG}(t) + J_{ex}(t) + G_{Kx}(V_m)\left(V_m(t) - E_K\right) + G_h(V_m)(V_m(t) - E_h) + \\ G_{Ca}(V_m)\left(V_m(t) - E_{Ca}\right) + G_{BK}(V_m, [Ca^{2+}])(V_m(t) - E_K) + G_{Cl(Ca)}(V_m, [Ca^{2+}])\times, \\ \times(V_m(t) - E_{Cl}) + I_{Na-K} + I_{PMCA} + G_L\left(V_m(t) - E_L\right) \end{aligned} \quad (13)$$

where G_{Kx}, G_h, G_{Ca}, G_{BK} and $G_{Cl(Ca)}$ are the conductances of depolarization activated potassium channels (K_x), hyperpolarization activated h channels, L-type Ca^{2+} channels (Ca_v), Ca^{2+} -activated K^+ (BK) and Cl^- channels, respectively. The E_Xs represent equilibrium or reversal

potential for each current. The two last terms are the Na-K ATPase and Ca^{2+} ATPase currents that can be regarded as constants, i.e. they are not significantly modulated by light or by changes in the V_m. The first term is the capacitive current of the cell membrane and the last term is a leak current with a voltage-independent leak conductance (G_L).

The model to simulate $J_{cG} + J_{ex}$ was already described in section 2.1.5 and the collected values for reversal potentials of each current component are presented in Table 1. The voltage-dependent conductances G_{Kx}, G_h and G_{Ca} can be modeled by Hodgkin Huxley (HH) formalism as in Liu & Kourennyi, (2004b). The Ca^{2+} -activated currents (I_{BK} and $I_{Cl(Ca)}$) can be described as Michaelis or Hill functions of $[Ca^{2+}]_i$ in the inner segment (see Liu & Kourennyi, 2004b). This requires modeling of the inner segment $[Ca^{2+}]_i$ that depends on the fluxes through L-type Ca^{2+} channels and PMCAs (see Liu & Kourennyi, 2004b). Although the models can qualitatively describe the V_m response to a flash of light, the stringent quantitative validation has not been completed. At present simulation of the mammalian rod V_m response is not possible because the data on the gating properties of the current mechanisms is insufficient. The behavior of the V_m in a rod's natural environment is further complicated by the interactions of the rod with other cells (electrical, chemical and ionic environment).

2.4 Transmission of rod V_m signal; the role of gap junctions

The V_m changes arising from photon absorptions are transmitted to second-order neurons by different mechanisms. The primary pathway includes rather slow metabotropic glutamatergic signaling to the depolarizing (ON) rod bipolar cells (DBC_r,). In many mammalian retinas rods are also known to be connected electrically to cones via gap junctions. (Raviola & Gilula, 1973; Kolb & West, 1977; Nelson, 1977; Schneeweis & Schnapf, 1995; Tsukamoto *et al.*, 2001). Thus, rods can transmit signals to the cone pathway (secondary rod pathway). In the primary pathway the light-induced hyperpolarization closes the L-type Ca^{2+} channels leading to a decline in $[Ca^{2+}]_i$ in the rod presynaptic terminal, because the PMCAs continue to extrude Ca^{2+} (see section 2.3.3). This leads to a decrease in the rate of glutamate release at the synaptic cleft (Rieke & Schwartz, 1996), which is sensed by glutamate receptors (mGlur6) in the DBC_rs (Nomura *et al.*, 1994). In the secondary pathway the change of the rod V_m is transmitted through gap junctions directly to cones that convey the signal to cone bipolar cells (BC_c) through ionotropic glutamate receptors (iGluRs, Morigiwa & Vardi, 1999; Haverkamp *et al.*, 2001).

General properties of gap junctions

Gap junctions are electrically conducting pores between adjacent cells that are formed by two hemichannels (connexons) linking the cytoplasms of neighbouring cells (for review, see Bloomfield & Volgyi, 2009). Hemichannels are comprised of six connexin proteins, which can be either similar (homomeric) or different isoforms (heteromeric). The pore of gap junctions can pass ions and small molecules whose molecular mass is below ~1 kDa. The conductance of gap junc-

tions can be modulated in several ways. One is phosphorylation of the hemichannel protein by protein kinases which has been shown to modulate the gap junction conductance. The kinase activity can be modulated by several factors e.g. by cAMP, cGMP and the Ca^{2+} sensor protein calmodulin. Increasing intracellular Ca^{2+} or protons usually decrease the gap junction conductance. However, the conductance of the gap junctions formed by Cx36 connexins is actually increased upon acidification. Light has been shown to modulate the gap junction conductance in retinal amacrine and horizontal cells (Bloomfield *et al.*, 1997; Xin & Bloomfield, 1999). These light-dependent modulations are thought to be mediated by dopamine or nitric oxid (Mills & Massey, 1995).

Gap junctions between rods and cones

The cone hemichannel of the rod-cone gap junction is thought to be comprised of the connexin isoform Cx36 in the mouse whereas the hemichannel in the rods remains unknown (see Bloomfield & Volgyi, 2009). Through gap junctions, rods utilize the cone signaling pathway to transmit visual information sensed by rods. When gap junctions between rods and cones are open, the rod membrane potential strongly affects the cone V_m (Schneeweis & Schnapf, 1995). I.e. the hyperpolarization of rods by light spreads to cones. Thus, the closure of gap junctions would relieve cones from the hyperpolarizing effect of rods and allow cones to function over a wider range of V_m. Differently from cones, the rod membrane potential is not much influenced by the cone V_m at least in the peripheral retina of primates (Schneeweis & Schnapf, 1995) or in the mouse retina where cones outnumber rods. The gap junctions between rods and cones are controlled by a circadian clock (Ribelayga *et al.*, 2008). During night the gap junctions are open allowing the rods to use the cone pathway. In the daytime the release of dopamine leads to closure of gap junctions possibly through cAMP-dependent phosphorylations of connexins (Ribelayga & Mangel, 2010).

3. Aims of the study

The general objective of this thesis was to investigate the role of certain ionic mechanisms involved in the generation and transmission of electrical signals in the mouse rod photoreceptor. The main emphasis was put on mechanisms modulated by changes in the intracellular concentration of divalent cations and/or by light. All the studies included in this thesis were conducted by recording the photoreceptor component (fast PIII) of transretinal ERG from isolated mouse retinas. The detailed objectives were:

1. *To identify the molecular mechanism(s) that generates the fast peak component present in the electroretinogram (ERG) responses to bright flashes of light* (paper I). The ERG signal consists of field potentials rising from the electrical activity of the cell membranes in the retina. The leading edge of the a-wave of the ERG response is generally thought to linearly reflect the changes in the outer segment current of rod photoreceptors. However, the ERG responses of some mammalian rods to bright flashes contain a fast peak component whose molecular origin has remained unknown. The goal of this work was to identify the molecular mechanism or mechanisms generating this component. A further objective was to find out whether the peak component compromises the assumption about the linear relation between J_{cG} and the leading edge of the a-wave of the ERG response.

2. *To find out whether the PDE* lifetime (τ_E) is modulated by intracellular Ca^{2+} in mouse rods* (paper II). Earlier data have mostly indicated that the deactivation of PDE* molecules is rate-limiting for the recovery kinetics of WT mouse rod flash responses. Based on data from amphibian rods, this rate-limiting recovery reaction was originally thought to be independent of background light. Recent data, however, suggests that τ_E of mouse rods is modulated by light. The molecular mechanism for this feedback has remained unknown. The Ca^{2+} ion is a natural candidate for this modulation, and the goal was to find out whether the changes in $[Ca^{2+}]$ can modulate τ_E.

3. *To investigate the specificity of the calcium (Ca^{2+}) sensor proteins recoverin and GCAP to divalent cations* (paper III). It is generally believed that the molecules mediating Ca^{2+} signals are very specific, being able to discriminate Ca^{2+} from other ions very effectively. This view is based on the fact that the Ca^{2+} sensor proteins must detect small changes in $[Ca^{2+}]_i$ in the presence of ~10^4 – 10^5 –fold higher concentration of the chemically very similar divalent cation Mg^{2+}. The primary origin of this high selectivity of Ca^{2+} over Mg^{2+} is

thought to arise from the smaller size of Mg^{2+} (r_i = 0.72 Å) compared to Ca^{2+} (r_i = 1.00 Å). The goal in this study was to test the functionality, and thus the selectivity of the EF-hands, of the rod calcium sensor proteins recoverin and GCAP in their natural cellular environment when Ca^{2+} is replaced with other divalent metal ions. To test whether the specificity of the Ca^{2+} binding sites in GCAP and recoverin is strictly determined by the ionic radius, studies were focused on Co^{2+} with an ion radius r_i = 0.75 Å (high spin) or 0.65 Å (low spin) close to that of Mg^{2+}.

4. To *find out whether the gap junction conductance between rods and cones can be modulated by light-dependent mechanisms located in the photoreceptors* (paper IV). Earlier data suggests that the rods and cones in mammalian and fish retinas are electrically coupled through gap junctions during night, and that this electrical connection is cut off at the daytime. There is evidence that the extent of rod-cone coupling is controlled by a circadian clock acting through a slow dopamine-dependent hormonal pathway. The objective of this work was to determine whether the gap junction conductance can be controlled by light through mechanisms that are located entirely in the photoreceptors themselves.

4. Methods

The electrical responses of rod photoreceptors to light can be recorded with several methods. Their outer segment current can be directly measured with suction electrodes (Baylor *et al.*, 1979) and their membrane voltage can be recorded with intracellular or patch electrodes. The outer segment current is dominated by the CNG channel current J_{cG} which reflects directly the cGMP homeostasis and dynamics in the ROS whereas V_m is also affected by the voltage-gated conductances of the inner segment. The generation and transmission of electrical signals in rods can be also studied with electroretinogram (ERG), *i.e.* by measuring the potential changes on the surface of the eye of a living animal (*in vivo* ERG) or the voltage across an isolated retina (transretinal or *ex vivo* ERG). The electrophysiological research of this thesis required long experiments with stimulus protocols and manipulations severely straining to the photoreceptor cells. Therefore recording of the photoreceptor component of the transretinal ERG (fast PIII, see below) from the intact isolated retina was chosen for the experimental method. This approach was deemed most suitable for the following reasons: (1) it allowed long and stable experiments, (2) provided a relatively physiological environment for rods, (3) enabled easy manipulation of the ionic environment around the whole rod, and (4) offered superior signal-to-noise ratio compared to the other electrophysiological techniques.

4.1 Transretinal electroretinogram (*ex vivo* ERG)

In the *ex vivo* ERG the reference potential is that of the distal side of the retina, i.e the changes in the voltage $U = V_P - V_D$ (Figure 4A) are measured. This voltage exists because extracellular radial dipole currents are formed between spatially separated (in radial direction) current sources and sinks in the retinal cell membranes. Figure 4B shows *ex vivo* ERG responses to flashes of light recorded from a mouse retina. The responses start with a negative a-wave followed by a positive b-wave. It is generally accepted that the initial negative-going leading edge of ERG recorded from a dark-dapted retina originates from the action of photoreceptors and the b-wave is thought to arise mainly from the electrical activity of the rod bipolar cells (e.g. Pugh, Jr. *et al.*, 1998). The b-wave can be abolished by blocking glutamatergic synaptic transmission to reveal the PIII component as an extension of the a-wave (Granit, 1933; shown in Figure 4C). The PIII component is composed of the photoreceptor response (fast PIII), and a slow negative wave (slow PIII). The slow PIII is generated by the current sinks and sources in the Müller cells. It can be removed

by inhibiting the K^+ currents of the Müller cells by Ba^{2+} (Bolnick *et al.*, 1979), leaving only the fast PIII as demonstrated in Figure 4D for the mouse retina.

The basic principle of how the fast PIII is generated in the photoreceptors is quite well understood. In darkness, a cation (mainly K^+) efflux through the photoreceptor inner segment plasma membrane channels is balanced by an equal charge influx mainly through the outer segment CNG channels (Hagins *et al.*, 1970;Penn & Hagins, 1972). Consequently, a radial dipole current (or a circulating dark current) between the inner segment current source and the outer segment current sink is formed. Light decreases the CNG channel current and the subsequent hyperpolarization of the cell membrane reduces the outflow of K^+ through potassium channels. Consequently, the radial dipole current between the inner and outer segment region is reduced and this is observed as a negative-going leading edge of the ERG signal. However, the fast PIII responses of some mammalian species also contain features not explained by this simple framework, such as the transient negative peak component clearly present in the *ex vivo* ERG responses recorded from the mouse retina (Figure 4D). The molecular mechanisms behind this component, as well as its consequences to the interpretation of the ERG light responses were studied in paper I and are further discussed in sections 5.1 and 6.1.

4.2 Experimental methods

4.2.1 Retina preparation and measurement conditions

All recordings were done from freshly isolated, dark-adapted mouse retinas. The retinas were detached in a modified Ringer's medium supplemented with L-15 and buffered to pH 7.5 with HEPES. The medium used during preparations was usually cooled to ca. + 4°C. The whole retina was isolated from the eye under dim red light, trying to minimize the physical contacts between the dissection instruments and the retina. Figure 5A illustrates the method used to isolate the mouse retina. The eye was first opened along the equator with fine scissors, and the lens was removed with tweezers yielding an "eye cup" with the retina still attached (see the left panel in Figure 5). Then starting at some point at the equator a cut with scissors was made towards the optic nerve located approximately at the pole of the eye cup. This cut was made carefully between the sclera and the retina to keep the retina as intact as possible. Now the sclera and other layers of the eye around the retina could be withdrawn with two tweezers to reveal the whole retina (see center and right panel of Figure 5A). Quite often, but not always, the final detachment of the retina required a disconnection of the optic nerve by scissors.

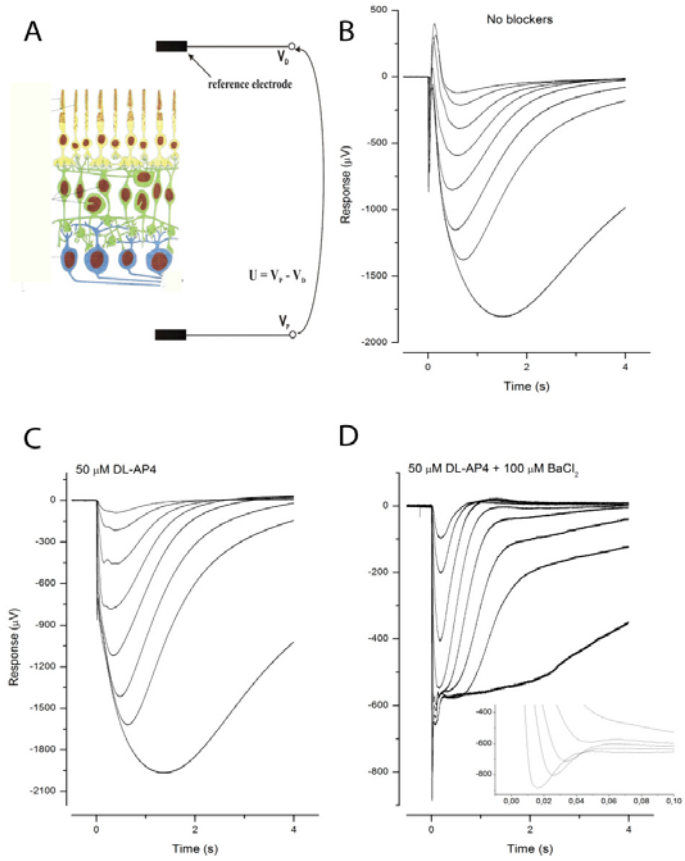

Figure 4 Signal components in the mouse transretinal ERG. (A) In transretinal ERG changes of voltage $U = V_P - V_D$ are measured. (B) Transretinal ERG responses to flashes of light producing 4 - 60 000 R*s recorded in physiological medium without blockers of synaptic transmission or channels. (C) PIII responses of the same retina to identical stimuli as in B after isolation with 50 μM DL-AP4. (D) Fast PIII responses of the retina in B and C to identical stimuli, isolated with 50 μM DL-AP4 and 100 μM $BaCl_2$.

Most of the experiments for papers I-III were done at 25°C but some control experiments were also conducted at 37°C, as were all the experiments for paper IV. At both temperatures modified Ringer's solution supplemented with L-15 was used for perfusion. An important factor determining the stability of recordings was the renewal rate of the medium around the retina. The higher metabolism at 37°C required also a faster perfusion rate. The volumetric flow rate (Q) of 1.4 mL min^{-1} at 25°C and to 4 – 5 mL min^{-1} at 37°C (these flow rates correspond to an exchange rate of the medium of about 1 – 10 s^{-1} above the effective recording area of the retina) provided stable responses in our recording geometry (see below).

4.2.2 Recording and light stimulation

A schematic view of the recording setup is presented in Figure 5B. The retina was placed in the specimen holder that was in a light tight Faraday cage during the measurements. The retina laid flat-mounted photoreceptor side upwards on a porous black filter paper. The proximal side of the retina was electrically connected to an Ag/AgCl pellet electrode through a 0.5 mm diameter hole under the filter paper, re-

straining the measurement area to the central part of the retina. A closed perfusion system provided a stable and fast flow of the perfusion solution over the distal side of the retina. The perfusion liquid was connected to the other macroscopic electrode and the voltage measured between the two electrodes was amplified, low-pass filtered with an 8-pole analog Bessel filter (f_c = 300 – 1000 Hz), and sampled at 1 - 10 kHz with 0.25 μV resolution. A differential amplifier placed in the Faraday cage was used as a preamplifier to minimize the noise from external sources. The Bessel-type filter was chosen because the delay it produces is almost frequency-independent across the entire passband, and therefore does not affect the shape of the measured signal. The temperature of the perfusing solution and the heat exchanger under the specimen holder were adjustable and the temperature of the retina was monitored with a small thermistor placed close to the retina.

An aperture on the top of the specimen holder restricted the light stimulation to the effective measurement area to minimize the interference of reflected light from the structures of the specimen holder. Light stimulation was produced by lasers and computer-controlled magnetic shutters and was guided with optic cable into the Faraday cage to produce a homogenous full-field illumination with light arriving almost parallel to the photoreceptor's longer axis.

4.2.3 Isolation of the rod and cone photoreceptor components (fast PIII)

The strategy for isolating the fast PIII component at 37°C was illustrated in Figure 4B-D. When experiments were conducted at 25°C, a somewhat different strategy was used to remove the b-wave and slow PIII. The b-wave was much less viable at 25°C than at 37°C probably because HEPES was used as the sole pH buffer at 25°C instead of complementing the bicarbonate-CO_2 buffering system used at 37°C (see also Azevedo & Rieke, 2011). At 25°C the b-wave was consistently abolished with 2 mM glutamate analog aspartate present to saturate the glutamatergic synaptic transmission. The slow PIII was removed by adding 10 mM $BaCl_2$ to the solution in the lower electrode space of the specimen holder (Nymark *et al*, 2005). This approach was adopted to effectively block the K^+ channels at the endfeet of the Müller cells at the proximal side of the retina while minimizing the effects on the K^+ channels of the photoreceptors continuously perfused with Ba^{2+} -free medium.

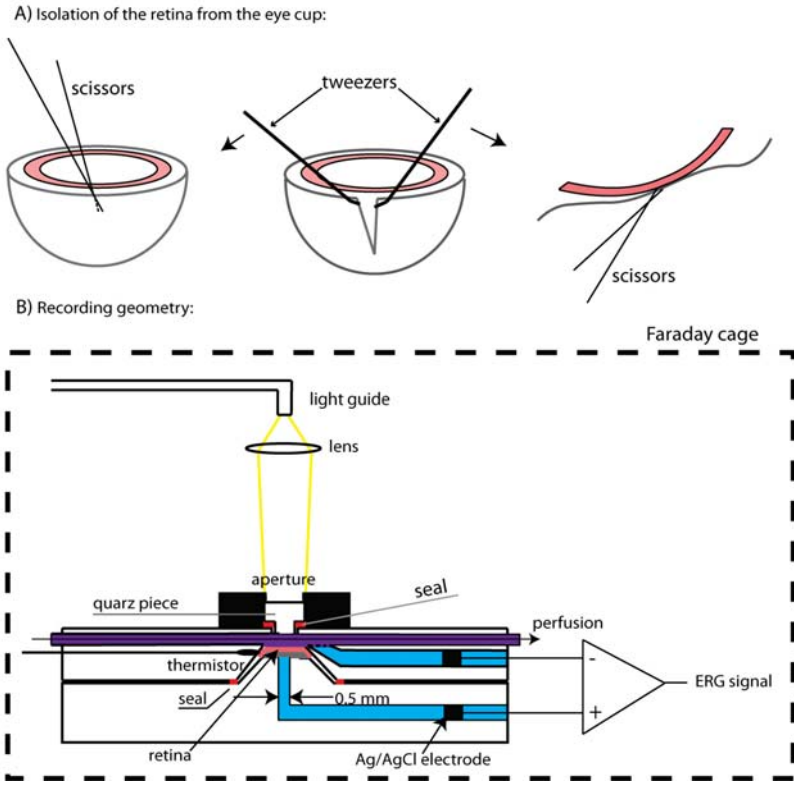

Figure 5 Experimental protocol and isolation of rod fast PIII. (A) Isolation of the retina. First the proximal hemisphere of the eye and the lens is removed as described in the text and an eye cup with the retina (left panel) is transferred to the Ringer solution. Then a single cut is made between retina and sclera with scissors and other layers except the retina are pulled away with two tweezers (center panel). The final isolation of the retina is obtained by cutting the optic nerve with scissors (right panel). (B) The isolated retina (pink) is placed in the specimen holder photoreceptors upwards.

The responses to three or four of the dimmest flashes in Figure 4D resemble qualitatively the corresponding outer segment current responses recorded with suction electrode from single mouse rods. However, the ERG response to bright flashes is more complex, and contains also a component generated by cone photoreceptors. The cone component was isolated with a pre-flash method (Heikkinen *et al.*, 2008), subtracted from the combined photoreceptor response in paper I and explicitly studied in paper IV. In the pre-flash method a strong flash is first given to saturate the rods, and a test-flash is delivered typically 0.5 s after the pre-flash when the rods are still saturated and the less sensitive cones have already recovered their prestimulus state. The small response elicited by the test-flash represents the cone fast PIII.

4.3 Experimental protocols and analysis

4.3.1 Studying the modulation of GC activity and shortening of τ_R by changes in Ca^{2+} or other divalent cations (paper III)

Acceleration of the GC activity and shortening of τ_R in response to the light-induced decline of $[Ca^{2+}]_i$ can be investigated with the step/flash paradigm (Fain *et al.*, 1989), in which steps of light of va-

rying intensity are followed by a bright flash presented simultaneously with extinction of the light step. The recovery of J_{cG} during the steps of light in the mouse rods is dominated by GCAP-mediated acceleration of the GC activity (Chen *et al.*, 2010b) and the acceleration of the flash response recovery when the intensity of the preceding light step is increased is thought to arise from the recoverin-mediated modulation of τ_R (Makino *et al.*, 2004; Chen *et al.*, 2010a). We recorded step/flash responses with the *ex vivo* ERG from intact mouse retinas to probe the dependence of GCAP and recoverin functionality in the presence Ca^{2+} or some selected divalent cations. The *ex vivo* ERG method allowed changing the ionic composition around the whole rod photoreceptor cell. This enabled reversible testing of whether a substitute divalent cation can function similarly to Ca^{2+} in modulating GC activity and/or shortening τ_R by switching between media containing either normal 1 mM [Ca^{2+}] or equimolar concentration of some other divalent cation with no Ca^{2+}. A convenient "reference solution" (containing low ~10^{-8} M free [Ca^{2+}]) in which Ca^{2+} feedback was disabled was used as a control condition (see Results and Discussion). The fact that a single *ex vivo* ERG response provided automatically an ensemble average from ~500 000 rods and an excellent signal-to-noise ratio facilitated greatly the use of step/flash protocol for the mouse rods.

4.3.2 Determining the amplification of the phototransduction activation reactions

The gain of phototransduction activation reactions was quantified by determining the amplification constant A (Lamb & Pugh, Jr., 1992, the LP model) from the responses to short flashes. A delayed Gaussian function

$$r(t) = r_{\max}\left(1 - \exp[-\tfrac{1}{2}\Phi A(t - t_d)^2]\right) \qquad (14)$$

was fitted to the leading edge of the measured fast PIII responses. There, r_{max} is the saturated rod response amplitude (measured at the peak of a flash response to bright flash, see Figure 4D) and t_d combines the delays of phototransduction reactions and measurement electronics. The choice of the maximal amplitude was somewhat arbitrary in the ERG flash responses (see paper I) and the amplification constant determined here might not accurately describe the absolute value of the molecular amplification. However, this choice yielded consistent results that could be also compared to the A determined at low very $[Ca^{2+}]_o$ when the nose is absent. It should be noted that the model's assumption regarding the sufficiently low level of [cGMP] in outer segment does not necessarily hold during the low Ca^{2+} treatment. Yet, the analysis was used to obtain a parameter that could be used for comparing the kinetics of activation reactions between physiological and low $[Ca^{2+}]_o$. A model that does not assume anything about the level of [cGMP] (see Appendix in paper III) was used to estimate how large an increase in [cGMP] under low $[Ca^{2+}]_o$ is needed to explain the observed change in the apparent A as determined with LP model.

4.3.3 Determining the rate constant of the slowest deactivation reaction in the phototransduction ($k_D = 1/\tau_D$)

The "Pepperberg analysis" (Pepperberg *et al.*, 1992) was applied to saturated fast PIII responses (Φ = 100 – 3000 R*) recorded from the intact mouse retina to determine the dominant time constant (τ_D). The method provided a possibility to quantitatively study the longer of the lifetimes of R* or PDE*. In mouse rods τ_D most probably corresponded to τ_E (see 2.1.2).

5. Results

5.1 Elucidation of the molecular mechanism(s) generating the nose component; implications to the linearity assumption between J_{cG} and the a-wave (paper I)

A fast peak component was identified in the pharmacologically isolated mouse fast PIII responses to bright light flashes. This component was similar to the "nose" component described by Arden (Arden, 1976) from the isolated rat retina. Subtraction of the cone contribution from the mixed rod and cone response did not remove the nose-like component, indicating that the nose is not generated by the cone activity but originates in the rods. The results of this thesis showed that the nose is generated primarily by the V_m -dependent h channel current of the rod photoreceptors. The contribution of the other known ion channels in the inner segment, the L-type Ca^{2+}, BK and Cl(Ca) channels, to the nose were excluded by pharmacological approaches. This strongly suggests that the Kx channel that could not be blocked may act as the current source in the generation of the nose component. To test whether the mechanisms generating the nose affect the leading edge of the responses to bright flashes, the h channel activity was removed with h channel blockers. The data from these experiments showed that the h channel activity does not contribute to the activation phase of photoresponses.

5.2 Large and stable photoresponses can be maintained at very low ~10^{-8} M $[Ca^{2+}]_o$ in *ex vivo* ERG (papers II and III)

One of the original goals for the investigations with lowered external $[Ca^{2+}]_o$ was to study whether a stable state with the calcium-dependent feedback mechanisms of phototransduction switched off could be found. In papers II and III rod fast PIII photoresponses under physiological 10^{-3} M and very low ~10^{-8} M $[Ca^{2+}]_o$ were compared. In darkness a steady state with large r_{sat} (reflecting large J_{cG}) was consistently achieved after *ca.* 5-15 min exposure to the low $[Ca^{2+}]_o$, especially at 25°C (Table 2). Initially after the switch to low $[Ca^{2+}]_o$, the saturated responses attained very large amplitudes (r_{sat} often exceeded 1 mV), and then declined to a stable value with r_{sat} still over 2-fold larger compared to under physiological $[Ca^{2+}]_o$. During the low Ca^{2+} exposures the feedback mechanisms controlling GC activity and τ_R were disabled as indicated by the absence of both response recovery during step illumination and acceleration of the saturating flash response recovery in the step/flash experiments. Table 2 combines the rod photoresponse parameters extracted from the fast PIII res-

ponses under physiological conditions and in 25 nM $[Ca^{2+}]_o$. Both the activation and deactivation phases of photoresponses were decelerated upon Ca^{2+} removal, leading to an apparent reduced gain of the activation reactions (as reflected by the amplification factor A), to a larger τ_D and to a longer time for single photon responses to reach the peak amplitude in low Ca^{2+} (t_p).

Table 2 Comparison of flash response parameters between normal 1 mM $[Ca^{2+}]_o$ and low 25 nM $[Ca^{2+}]_o$.

Condition	r_{sat} (μV)	A (s^{-2})	τ_D (ms)	t_p (ms)
Normal Ca^{2+} (37°C)	278 ± 78	16 ± 0.7	166 ± 12	152 ± 23
Low Ca^{2+} (37°C)	417 ± 45	1.4 ± 0.5	251 ± 15	210 ± 9
Normal Ca^{2+} (25°C)	151 ± 19	2.6 ± 0.3	342 ± 28	307 ± 18
Low Ca^{2+} (25°C)	353 ± 38	0.4 ± 0.1	662 ± 50	570 ± 60

5.3 A novel unidentified Ca^{2+} dependent mechanism controls the dominant time constant of the saturated mouse rod photoresponse recovery (paper II)

It was demonstrated that the time dominant constant τ_D of the saturated mouse rod photoresponse recovery can be robustly determined from rod fast PIII responses with the "Pepperberg analysis". The τ_D obtained from the intact mouse retinas under physiological $[Ca^{2+}]_o$ were similar to those extracted from recordings from single mouse rods (paper II and Table 2). It was found that the τ_D of mouse rods was 1.5 – 2-fold larger in very low ~10^{-8} M $[Ca^{2+}]_o$ compared to its value under physiological $[Ca^{2+}]_o$, whereas smaller decreases of $[Ca^{2+}]_o$ down to 10^{-6} M did not alter τ_D. Further investigations indicated that the increased τ_D under the low $[Ca^{2+}]_o$ is not caused by the large J_{cG} or the related increase of [cGMP] in the rod outer segments. Experiments with lowered extracellular sodium concentration suggest that the increased τ_D is not due to elevated intracellular Na^+ concentration. It was also shown that the high expenditure of ATP under the low Ca^{2+} conditions could not explain the increase in τ_D.

5.4 Accelerated cGMP synthesis can account for the decreased amplification constant in low $[Ca^{2+}]_o$ (paper III)

In low Ca^{2+} the [cGMP] in the outer segment is elevated in darkness due to the acceleration of GC activity. Although the elevated [cGMP] could not explain the increase of τ_D under very low $[Ca^{2+}]_o$, it seemed possible that large [cGMP] might be the cause for the deceleration of the activation phase of the photoresponses (i.e. the apparent decrease in the amplification factor A) observed in low Ca^{2+}. Simulations with a phototransduction model showed that if an increase of [cGMP] from 4 μM in physiological $[Ca^{2+}]_o$ to 10 – 40 μM in low $[Ca^{2+}]_o$ was assumed, the model could explain the apparent decrease of the amplification constant observed in low Ca^{2+} (Table 2). This simulation result was supported by experiments (data not shown), in which the level of cGMP during low Ca^{2+} exposures was decreased with background light: under physiological $[Ca^{2+}]_o$ the leading edge of fraction-

al flash responses is known to be not affected by background light. However, if it were the high [cGMP] that compromises the apparent efficacy of the activation reactions in low Ca^{2+}, lowering the level of cGMP with background light should increase the apparent amplification constant during the low Ca^{2+} exposures. This was indeed observed.

5.5 Cobalt ion (Co^{2+}) appears to mediate the dynamic feedback signals that accelerate GC activity and shorten τ_R (paper III)

The EF-hand Ca^{2+} binding sites in calcium sensor proteins bind Ca^{2+} with much higher affinity compared to Mg^{2+}. This high specificity is thought to arise from the smaller size of the Mg^{2+} ion compared to that of Ca^{2+}. Further, binding of Mg^{2+} to the EF-hands does not induce the structural changes in the calcium sensor proteins needed to mediate the signal driven by binding of calcium ions. The ion specificity and functionality of the photoreceptor calcium sensor proteins GCAP and recoverin were investigated with the step/flash protocol. The initial hypothesis was that the Co^{2+} ion with ion radius very close to that of Mg^{2+} should not be able to mediate the dynamic feedback signals accelerating GC activity and shortening the R* lifetime that are normally driven by Ca^{2+}. Contrary to expectations, the response recovery during the steps of light present in physiological $[Ca^{2+}]_o$ and absent in low $[Ca^{2+}]_o$ was practically unchanged when Ca^{2+} was replaced with equal concentration of Co^{2+}. Similarly, the shortening of the starting time of the saturated flash response recovery in the step/flash protocol that is abolished in low $[Ca^{2+}]_o$ was present when Ca^{2+} was replaced with Co^{2+}.

5.6 Electrical coupling of rods and cones may be modulated by light-dependent mechanism located in the photoreceptor cells (paper IV)

There is evidence that in some species the gap junctional conductance between rods and cones can be controlled by a circadian clock. The results of this work showed that relatively dim background light, not expected to affect much the cone phototransduction (or stimulate the photosensitive ganglion cells of the inner retina), increased the cone fast PIII response amplitudes. A similar enhancement in the photopic (light-adapted) ERG a-wave during first minutes of constant light stimulation has been well recognized (Gouras & MacKay, 1989), but neither its origins or its dependence on the background light intensity have been known. In this paper the cone flash responses were studied with a rod-saturating preflash, so that cone light responses could be compared in darkness and under different background lights. The cone response enhancement by background light could be mimicked by application of three of the four tested gap junction antagonists to a dark-adapted retina. Also, all the tested gap junction blockers prevented light induced growth of the cone responses and did not enhance cone responses further when they were applied to the light-adapted retina. The results strongly suggest that (1) the growth of the photopic a-wave reflects growth in the cone photoreceptor light response (fast PIII) compared to the dark-adapted situation and (2) the increase of the cone fast PIII is caused by light-dependent modulation of the rods' signaling pathway through gap junctions to the cones.

6. Discussion

6.1 About the molecular mechanism of the nose component; implications to the determination of A and τ_D (papers I and II)

The electroretinogram (ERG) is a widely used tool to investigate the retinal function both in basic and clinical research. It offers an efficient and non-invasive way to study e.g. phototransduction and mouse models of hereditary eye diseases. Although more than a century has past from one of the first ERG recordings by Holmgren in 1865 (reviewed in Armington, 1974), the molecular mechanisms of the ERG signal components still remain partly unknown. One of the most prominent ERG signal components that has remained unexplained is the nose component in the fast PIII responses to bright flashes recorded from certain mammalian species, either from isolated retinas (rat: Arden, 1976; Green & Kapousta-Bruneau, 1999; Nymark *et al.*, 2005) or from intact anesthetized animals (cat: Kang Derwent & Linsenmeier, 2001, monkey: Jamison *et al.*, 2001). The nose component is also present in the pharmacologically isolated fast PIII responses recorded from the isolated mouse retinas. The importance of clarifying the mechanistic origin of the nose component comes from the fact that the nose component might mix with the leading edge of the ERG signal, generally believed to accurately reflect the changes in the light-sensitive outer segment current and widely used for determination of phototransduction amplification. Since earlier studies by others and the data of this thesis indicated that the nose is of rod origin, there are in principle two (main) possibilities how it can be generated in rods: (1) by capacitive currents (I_C) that are proportional to the rate of change of the V_m (Robson & Frishman, 2011) or (2) by a dipole current that is formed between a current source and a sink that are activated or modulated by the light-induced changes in V_m and the consequent changes in voltage-dependent currents through the rod plasma membrane. Several evidence spoke against the role of capacitive currents in generating the nose: (1) exposing rods to very low $[Ca^{2+}]_o$, a treatment that is not expected to change the capacitance of the rod plasma membrane, removed the nose, (2) the nose became visible already with rather low flash strengths (between 1000 and 2000 R*) that should not elicit substantial capacitive currents (see Penn & Hagins, 1972; Cobbs & Pugh, Jr., 1987; Breton *et al.*, 1994), and (3) blocking the h channels removed the nose. It is expected, however, that a capacitive nose-like component becomes visible with very strong and short flashes, especially at 37°C when dV_m/dt is high. It was concluded that the nose

component studied in this thesis is not significantly affected by I_C. The likely candidate for the molecular mechanism creating the sink of the dipole current that generates the nose component was identified (the h channel). The corresponding current source, however, remained unclear. The blockage of all the other known ion channels in the rod inner segment except the Kx channels did not remove the nose. It is not, however, self-evident that Kx current alone do mirror the h current in physiological conditions and thus act as the current source of the dipole responsible for the generation of the nose component. Indeed, also the Kx current creates an apparent sink as response to light hyperpolarizing the V_m. Consequently there is a net decrease in the outward K^+ current through Kx channels. Additionally, formation of the dipole current between the h and Kx channels (or the other possible channels acting as the source) requires that their spatial distribution along the rod inner segment would be different. At present there is, however, no quantitative data on channel distributions in the mouse rod inner segment.

In the present work the kinetics and gain (A) of the phototransduction activation and the dominant time constant τ_D of the saturated photoresponse recovery were determined from the fast PIII responses with the LP model and the "Pepperberg analysis", respectively. Since the nose might interfere with the linearity assumption between the leading edge of the fast PIII and J_{cG}, it appeared possible that the A determined from the fast PIII flash responses might not accurately reflect the underlying phototransduction reactions. The observation that h channel blockers removed the nose without affecting the leading edge of the mouse photoresponses strongly suggested that the nose is primarily generated by inner segment current(s) through voltage-gated h channels that are gated slowly enough not to interfere with the early phase of light responses. This idea is in agreement with earlier data from salamander rods demonstrating that the kinetics of the leading edges of the V_m and J_{cG} flash responses are remarkably similar (Baylor *et al.*, 1984). Therefore it was concluded that the mechanisms behind the nose do not affect the value of the amplification factor determined from the early phases of mouse rod ERG photoresponses.

The determination of the dominant time constant τ_D of saturated photoresponse recovery has been successfully used in single-cell current recordings to investigate the slowest or the rate-limiting deactivation reaction of phototransduction shut-off. The power of the determination of τ_D is that it gives the rate constant ($k = 1/\tau_D$) of this reaction in the intact photoreceptor cell, i.e. in maximally physiological conditions. The recovery phase of fast PIII responses, however, is affected by the voltage-gated channels in the inner segment plasma membrane, at first glance complicating the use of *ex vivo* ERG for τ_D determinations. As discussed more thoroughly in paper II, there are strong grounds to believe that the τ_D determined from the fast PIII ERG flash responses is insensitive to the voltage-dependent currents of the inner segment. The rationale for this is that the onset of the saturated photoresponse recovery is determined soon after the responses start to recover from a *common* plateau level, i.e. only the on-

set of photoresponse recovery varies over the stimulus range used for the analysis, while the slopes of recoveries remain unaltered. This ensures that even if some voltage-gated channels do shape the response recovery, they are expected to change the kinetics of every response equally and thus would not affect the determined value of τ_D. This reasoning is consistent with the experimental results of the current study giving a very similar τ_D at 37°C to the published values obtained with single cell recordings from single mouse rods.

6.2 Low $[Ca^{2+}]_o$ provides a stable reference state in which the Ca^{2+} feedback is disabled

Most of the research on the Ca^{2+}-dependent feedback mechanisms of phototransduction has relied on disabling these mechanisms either by (1) clamping $[Ca^{2+}]_i$ to its physiological steady state value in darkness or during background light, or (2) removing or changing the expression level of the protein molecules that participate in mediating the Ca^{2+} signals. With these approaches the role of different Ca^{2+} feedback mechanisms have been dissected by comparing responses to more or less standard light stimulus protocols (flashes, steps or step+flash stimuli) between the physiological state and under conditions where a selected feedback mechanism or mechanisms have been disabled. In the present work one aim was to investigate the functional properties and ion specificity of the Ca^{2+} sensor proteins GCAP and recoverin (paper III). For that purpose it was highly desirable to find a stable and reversible reference state (preferably lasting several tens of minutes) in which the Ca^{2+} feedback is disabled but the relevant Ca^{2+} sensor proteins present and functional. Indeed, it was found that when $[Ca^{2+}]_o$ were lowered to ~10^{-8} M, stable and large responses could be recorded in the intact retina. The lack of all hallmarks of acceleration of GC activity or shortening of τ_R in response to appropriate light stimuli indicated that the dynamic Ca^{2+} feedback mechanisms were completely disabled (see Results). Further, the original (prior to the low Ca^{2+} exposure) size and shape of the light responses could be restored by switching back to normal 1 mM $[Ca^{2+}]_o$.

The stable and reversible state of rods in the low $[Ca^{2+}]_o$ enabled switching between the physiological conditions with Ca^{2+} feedback enabled and a reference condition with Ca^{2+} feedback disabled. Thus the effects of Ca^{2+} feedback removal could be compared against the control light responses from the same preparation, as a clear advantage over the genetic approach where statistics has to be collected from different animal populations. Moreover, due to the reversibility of the low $[Ca^{2+}]_o$ treatment, it was also possible to use this state as a reference state in testing e.g. how other divalent cations could replace Ca^{2+} in mediating the negative feedback signals. However, while the low $[Ca^{2+}]_o$ seemed like a good reference state, some features of the rod light responses appeared anomalous. Especially, the apparently decelerated kinetics of the phototransduction activation reactions (as judged by the decreased A determined using the LP model) and the consequent low flash sensitivity of rods under low $[Ca^{2+}]_o$ seemed at first strange since the activation coefficient A is thought to be independent of $[Ca^{2+}]_i$. However, modeling of the flash responses indi-

cated that the accelerated synthesis rate of cGMP by GCs under low $[Ca^{2+}]$ can account for the observed decrease of the apparent amplification factor without assuming any modulation of the molecular amplification of the activation reactions between the normal and low Ca^{2+} conditions ($A = \nu_E \beta_{sub} n_{cG}$).

Another interesting phenomenon not explained by the current framework of rod phototransduction was the decelerated response recovery kinetics during low $[Ca^{2+}]_o$ perfusion, exemplified by the increase in the dominant time constant of flash response recovery as inferred by the Pepperberg analysis from the saturated flash responses (paper II). The results of the current study strongly suggest that this cannot be explained by the increased [cGMP] during low $[Ca^{2+}]_o$ exposures. Also, the possible side effects caused by the boosted J_{cG} and the subsequent accumulation of $[Na^+]$ into the ROS as well as the high expenditure of ATP in very low $[Ca^{2+}]_o$ were excluded as possible explanations for the increased τ_D. It seems very unlikely that τ_R would be increased so much that it could switch to the dominant time constant of response recovery in very low Ca^{2+}. This is even more so, since a decrease in $[Ca^{2+}]_i$ is known to shorten the R* lifetime, not increase it. Therefore it feels natural to assume that the increased τ_D in very low $[Ca^{2+}]_o$ indicates lengthening of τ_E. The increase in τ_D could not be seen until $[Ca^{2+}]_o$ was lowered below 10^{-6}– 10^{-7} M. With these $[Ca^{2+}]_o$ values (close to the physiological value of $[Ca^{2+}]_i$ in the ROS), the NCKXs can probably drive $[Ca^{2+}]_i$ below the levels that can be attained in bright light. Thus this effect of decelerated photoresponse deactivation is not likely to be encountered under physiological conditions. Yet, it is clearly important to maintain $[Ca^{2+}]_i$ at an appropriate level to set the physiological kinetics of the rate-limiting deactivation reaction.

The mechanism that caused the increase in τ_D under very low $[Ca^{2+}]_o$ could not be found. At the moment the mechanism leading to increased τ_D under low $[Ca^+]_o$ conditions can be only speculated about. One obvious consequence of the very low calcium level is that the average net charge of the calcium sensor proteins is shifted towards negative charges and practically all recoverin molecules are expected to be solubilized. One candidate explanation for the increased τ_D might be some kind of interaction between the molecules involved in the deactivation of PDE* and the Ca^{2+}-free form of recoverin. Similar arguments can be used for the possible role of calmodulin and other calcium sensor proteins. One source of a plethora of possible explanations is the altered screening of the negative surface charges of membranes and proteins, while these are clearly beyond the current study.

6.3 Selectivity properties and functionality of EF-hand proteins in intact rods

Recoverin and GCAP belong to a large family of EF-hand proteins that mediate Ca^{2+} signals. One prominent feature of the Ca^{2+} sensor proteins is their high specificity for Ca^{2+} against other cations abundant in cells, including Mg^{2+} which is chemically very similar to Ca^{2+}. More specifically, the affinity of the EF-hand binding sites for Ca^{2+} is

generally much higher than for the 10^4 - 10^6 -fold more abundant Mg^{2+}. In addition, the (low probability) binding of an Mg^{2+} ion usually leads to a different conformation than binding of Ca^{2+}, which also contributes to the functional selectivity of the calcium binding proteins (see below). The physical factors determining the high specificity of the EF-binding sites have been mainly studied *in vitro* under conditions that might be far from those in the intact cells. Thus the correspondence of the results to the physiological function remains unclear. Therefore it would be of great interest to study the functional selectivity of the EF-hand Ca^{2+} sensor proteins under their natural cellular environment. Finding a cation that could replace Ca^{2+} in some specific Ca^{2+} signaling mechanism but discriminated by other Ca^{2+} dependent processes might open possibilities e.g. to dissect the relevance of different Ca^{2+} feedback mechanisms in phototransduction, or might have potential as a therapeutic substance.

Although the selectivity of the EF-hand Ca^{2+} binding sites over Mg^{2+} has been investigated extensively, not much is known about their specificity against other divalent cations. The chemical properties of Ca^{2+} and Mg^{2+} are very similar, and therefore the specificity of the calcium binding sites is thought to arise from the different physical size of these ions. Mg^{2+} is a small ion and its hydration energy is large compared to Ca^{2+}. Thus, the energy cost of dehydration upon binding an Mg^{2+} ion is larger than for Ca^{2+}. Due to its smaller diameter, Mg^{2+} prefers six-coordinated octahedral coordination geometry, while the EF-hand Ca^{2+} binding site is optimized for seven-coordinated pentagonal bipyramidal coordination geometry (Gifford *et al.*, 2007). Indeed, it has been shown that Mg^{2+} adopts octahedral coordination geometry in many EF-hand binding sites, which for example in recoverin appears to yield a conformation that cannot perform the same physiological function as binding of Ca^{2+} (Ozawa *et al.*, 2000). The results of paper III challenged the hypothesis about the ion size as the main determinant of selectivity by proposing that Co^{2+} can mediate the dynamic feedback through GC activity and R* lifetime control that are normally driven by Ca^{2+} in ROS. As the ion radius of Co^{2+} is very close to that of Mg^{2+}, the question arises: Why Mg^{2+} but not Co^{2+} could be discriminated by the EFh Ca^{2+} binding sites? The physiological data of paper III does not answer this question, and further studies are needed to clarify the selectivity mechanisms of the EF-hand Ca^{2+} binding sites. Both physiological data regarding physically and chemically different divalent cations and structural data with different *in vitro* techniques augmented with molecular modeling studies would be helpful in resolving this issue.

Rod phototransduction provided a convenient model system for studying the functional properties of Ca^{2+} signaling proteins in their cellular environment. It is an intrinsic property of this approach that to observe the dynamic feedback mediated by any divalent cation, the concentration of that divalent cation in the ROS must be modulated similarly to $[Ca^{2+}]_i$. Although the CNG channel is not very selective and most divalent cations can permeate into the ROS, the only divalent cation the NCKX is known to extrude in addition to Ca^{2+} is Sr^{2+} (Yau & Nakatani, 1984). The results of the present work clearly sug-

gest that the NCKX can extrude also Co^{2+}. As noted above, it would be relevant to screen the specificity of GCAP and recoverin against other divalent cations besides Co^{2+}. It was also observed that Sr^{2+} can drive the feedback mechanisms much like Ca^{2+} and Co^{2+} in the step/flash experiments (data not shown). This was not very surprising since Sr^{2+} is chemically and physically very similar to Ca^{2+}, and is often used as a substitute for Ca^{2+} in ion channel studies. However, many divalent cations cannot be extruded by NCKX even though they can permeate the CNG channel. Thus the concentration of these ions in the ROS will reach a steady level, and these ions cannot mediate the dynamic feedback processes. However, in the current study a potential method for testing whether these ions can bind to GCAP and reduce GC activity was found. It is based on the conclusion (see 5.4) that without Ca^{2+} or in very low Ca^{2+} the GC activity and thus the intracellular [cGMP] increase so much that the apparent amplification constant goes down. If the substitute cation could inhibit GC activity, it should be able to restore the physiological value of A.

It seems that although Nature has developed the EF-hand binding sites to be highly specific for Ca^{2+} over Mg^{2+}, the EF-hands do not necessarily exhibit similar selectivity over divalent cations present only as trace elements in cells. It is also somewhat surprising from a general point of view that a transition metal can mediate a dynamic signal: Typically transition metals are structural parts of biological molecules with covalency involved in the bonds, e.g. cobalt is known to be an integral part of vitamin B_{12}. The results also underline the differences between the selectivity mechanisms of various Ca^{2+} dependent processes. Although cobalt seems to be not discriminated by the EF-hand binding site, it can hardly permeate e.g. the voltage-gated L-type Ca^{2+} channels in rods, and it is actually used as a general Ca^{2+} channel inhibitor.

6.4 About the molecular mechanism regulating the gap junction conductance between rods and cones

A possible scheme for the proposed, rather surprising, connection between modulation of the rod-cone gap junctions and the long-known phenomenon of the growth in the light-adapted ERG is as follows: In darkness the hyperpolarization of the rod V_m by the pre-flash, that is used to saturate the rods to isolate the cone fast PIII (or in the more conventional approach, application of a steady, rod-saturating background light), spreads also to the cones. Consequently, the maximal change of the cone V_m that can be elicited by the test flash is restricted because the cone V_m is already hyperpolarized by the pre-flash. This is then manifested also as a decreased cone fast PIII response because e.g. the K^+ current that is part of the cone circulating current is decreased by the cone membrane hyperpolarization. Following a constant light stimulation, the gap junction conductance decreases (with a time constant of about 1 minute), and thus the rod V_m hyperpolarization by the pre-flash does not affect the cone V_m anymore. Subsequently, the pre-flash isolated cone fast PIII responses increase.

Earlier data have suggested that rods and cones of some species are electrically coupled at night and decoupled during the daytime (Ribelayga *et al.*, 2008). This would allow rods a direct and fast access to the cone pathways under low light conditions when the cones are generally inactive. The modulation of the gap junctional coupling between the two photoreceptor types is thought to be mediated by a dopamine-dependent hormonal pathway controlled by the circadian clock (Ribelayga & Mangel, 2010). The evidence from the present work suggests that the molecular pathway controlling the light-dependent modulation of the gap junctions between rods and cones is located entirely in the rod photoreceptors themselves: (1) already quite dim constant stimulation that is not expected to stimulate much the cones or light-sensitive ganglion cells in the retina could initiate the cone response enhancement, and (2) the experiments were conducted under conditions in which all glutamatergic transmission between photoreceptors and other retinal neurons was inhibited. The molecular mechanism that controls the proposed light-dependent modulation of the gap junctional coupling of rods and cones remains unknown. It has been suggested that the dopamine mediated modulation of the gap junctions between rods and cones is implemented by cAMP-dependent phosphorylation of the connexins (Li *et al.*, 2009). It is possible that also direct light-dependent modulation of the rod-cone coupling is achieved through the same molecular mechanism. In support of this hypothesis, [cAMP] has been shown to be modulated independently by dopamine and light in mammalian photoreceptors (Cohen & Blazynski, 1990; Nir *et al.*, 2002).

7. Conclusions

1. The h and most likely Kx channels, but not BK, L-type Ca^{2+} or Cl(Ca) channels, in the rod inner segment contribute to the generation of the peak component (the nose) in the mouse fast PIII response to bright flash.

2. The leading edge of the fast PIII flash responses is not affected by the ionic mechanisms generating the nose component.

3. Ca^{2+} is needed to set the physiological kinetics of the rate-limiting recovery reaction in mouse rods.

4. The Co^{2+} ion can mediate the Ca^{2+}-controlled negative feedback mechanisms that accelerate the GC activity through GCAP and shorten τ_R in the intact mouse rod photoreceptors.

5. The electrical coupling between rods and cones in the mouse retina might be closed by light by a mechanism located in the rod photoreceptor cells.

Reference List

Altimimi HF & Schnetkamp PP (2007). Na+/Ca2+-K+ exchangers (NCKX): functional properties and physiological roles. *Channels (Austin)* **1**, 62-69.

Ames JB, Dizhoor AM, Ikura M, Palczewski K, & Stryer L (1999). Three-dimensional structure of guanylyl cyclase activating protein-2, a calcium-sensitive modulator of photoreceptor guanylyl cyclases. *Journal of Biological Chemistry* **274**, 19329-19337.

Ames JB, Hamasaki N, & Molchanova T (2002). Structure and calcium-binding studies of a recoverin mutant (E85Q) in an allosteric intermediate state. *Biochemistry* **41**, 5776-5787.

Ames JB, Ishima R, Tanaka T, Gordon JI, Stryer L, & Ikura M (1997). Molecular mechanics of calcium-myristoyl switches. *Nature* **389**, 198-202.

Ames JB, Levay K, Wingard JN, Lusin JD, & Slepak VZ (2006). Structural basis for calcium-induced inhibition of rhodopsin kinase by recoverin. *Journal of Biological Chemistry* **281**, 37237-37245.

Arden GB (1976). Voltage gradients across the receptor layer of the isolated rat retina. *Journal of Physiology* **256**, 333-360.

Armington JC (1974). *The Electroretinogram* Academic Press, New York.

Arshavsky VY & Bownds MD (1992). Regulation of deactivation of photoreceptor G protein by its target enzyme and cGMP. *Nature* **357**, 416-417.

Attwell D (1986). The Sharpey-Schafer lecture. Ion channels and signal processing in the outer retina. *Quarterly Journal of Experimental Physiology* **71**, 497-536.

Attwell D, Borges S, Wu SM, & Wilson M (1987). Signal clipping by the rod output synapse. *Nature* **328**, 522-524.

Attwell D & Wilson M (1980). Behaviour of the rod network in the tiger salamander retina mediated by membrane properties of individual rods. *Journal of Physiology* **309**, 287-315.

Azevedo AW & Rieke F (2011). Experimental protocols alter phototransduction: the implications for retinal processing at visual threshold. *Journal of Neuroscience* **31**, 3670-3682.

Bader CR, Bertrand D, & Schwartz EA (1982). Voltage-activated and calcium-activated currents studied in solitary rod inner segments from the salamander retina. *Journal of Physiology* **331**, 253-284.

Barnes S (1994). After transduction: response shaping and control of transmission by ion channels of the photoreceptor inner segments. *Neuroscience* **58**, 447-459.

Barnes S, Merchant V, & Mahmud F (1993). Modulation of transmission gain by protons at the photoreceptor output synapse. *Proceedings of the National Academy of Sciences of the United States of America* **90**, 10081-10085.

Bastian BL & Fain GL (1982). The effects of low calcium and background light on the sensitivity of toad rods. *Journal of Physiology* **330**, 307-329.

Baumann L, Gerstner A, Zong X, Biel M, & Wahl-Schott C (2004). Functional characterization of the L-type Ca2+ channel Cav1.4alpha1 from mouse retina. *Investigative Ophthalmology & Visual Science* **45**, 708-713.

Baylor DA, Lamb TD, & Yau KW (1979). The membrane current of single rod outer segments. *Journal of Physiology* **288**, 589-611.

Baylor DA, Matthews G, & Nunn BJ (1984). Location and function of voltage-sensitive conductances in retinal rods of the salamander, Ambystoma tigrinum. *Journal of Physiology* **354**, 203-223.

Beech DJ & Barnes S (1989). Characterization of a voltage-gated K+ channel that accelerates the rod response to dim light. *Neuron* **3**, 573-581.

Bloomfield SA & Volgyi B (2009). The diverse functional roles and regulation of neuronal gap junctions in the retina. *Nature Reviews Neuroscience* **10**, 495-506.

Bloomfield SA, Xin D, & Osborne T (1997). Light-induced modulation of coupling between AII amacrine cells in the rabbit retina. *Visual Neuroscience* **14**, 565-576.

Bolnick DA, Walter AE, & Sillman AJ (1979). Barium suppresses slow PIII in perfused bullfrog retina. *Vision Research* **19**, 1117-1119.

Breton ME, Schueller AW, Lamb TD, & Pugh EN, Jr. (1994). Analysis of ERG a-wave amplification and kinetics in terms of the G-protein cascade of phototransduction. *Investigative Ophthalmology & Visual Science* **35**, 295-309.

Brown JE & Pinto LH (1974). Ionic mechanism for the photoreceptor potential of the retina of Bufo marinus. *Journal of Physiology* **236**, 575-591.

Burns ME & Pugh EN, Jr. (2010). Lessons from photoreceptors: turning off g-protein signaling in living cells. *Physiology (Bethesda)* **25**, 72-84.

Calvert PD, Ho TW, LeFebvre YM, & Arshavsky VY (1998). Onset of feedback reactions underlying vertebrate rod photoreceptor light adaptation. *Journal of General Physiology* **111**, 39-51.

Capovilla M, Cervetto L, Pasino E, & Torre V (1981). The sodium current underlying the responses of toad rods to light. *Journal of Physiology* **317**, 223-242.

Caruso G, Khanal H, Alexiades V, Rieke F, Hamm HE, & DiBenedetto E (2005). Mathematical and computational modelling of spatio-temporal signalling in rod phototransduction. *IEE Proceedings Systems Biology* **152**, 119-137.

Cervetto L, Lagnado L, Perry RJ, Robinson DW, & McNaughton PA (1989). Extrusion of calcium from rod outer segments is driven by both sodium and potassium gradients. *Nature* **337**, 740-743.

Chen CK, Burns ME, He W, Wensel TG, Baylor DA, & Simon MI (2000). Slowed recovery of rod photoresponse in mice lacking the GTPase accelerating protein RGS9-1. *Nature* **403**, 557-560.

Chen CK, Burns ME, Spencer M, Niemi GA, Chen J, Hurley JB, Baylor DA, & Simon MI (1999). Abnormal photoresponses and light-induced apoptosis in rods lacking rhodopsin kinase. *Proceedings of the National Academy of Sciences of the United States of America* **96**, 3718-3722.

Chen CK, Inglese J, Lefkowitz RJ, & Hurley JB (1995a). Ca(2+)-dependent interaction of recoverin with rhodopsin kinase. *Journal of Biological Chemistry* **270**, 18060-18066.

Chen CK, Woodruff ML, Chen FS, Chen D, & Fain GL (2010a). Background light produces a recoverin-dependent modulation of activated-rhodopsin lifetime in mouse rods. *Journal of Neuroscience* **30**, 1213-1220.

Chen J, Makino CL, Peachey NS, Baylor DA, & Simon MI (1995b). Mechanisms of rhodopsin inactivation in vivo as revealed by a COOH-terminal truncation mutant. *Science* **267**, 374-377.

Chen J, Woodruff ML, Wang T, Concepcion FA, Tranchina D, & Fain GL (2010b). Channel modulation and the mechanism of light adaptation in mouse rods. *Journal of Neuroscience* **30**, 16232-16240.

Cheng H, Aleman TS, Cideciyan AV, Khanna R, Jacobson SG, & Swaroop A (2006). In vivo function of the orphan nuclear receptor NR2E3 in establishing photoreceptor identity during mammalian retinal development. *Human Molecular Genetics* **15**, 2588-2602.

Cia D, Bordais A, Varela C, Forster V, Sahel JA, Rendon A, & Picaud S (2005). Voltage-gated channels and calcium homeostasis in mammalian rod photoreceptors. *Journal of Neurophysiology* **93**, 1468-1475.

Cobbs WH & Pugh EN, Jr. (1987). Kinetics and components of the flash photocurrent of isolated retinal rods of the larval salamander, Ambystoma tigrinum. *Journal of Physiology* **394**, 529-572.

Cohen AI & Blazynski C (1990). Dopamine and its agonists reduce a light-sensitive pool of cyclic AMP in mouse photoreceptors. *Visual Neuroscience* **4**, 43-52.

Corey DP, Dubinsky JM, & Schwartz EA (1984). The calcium current in inner segments of rods from the salamander (Ambystoma tigrinum) retina. *Journal of Physiology* **354**, 557-575.

Cornwall MC & Fain GL (1994). Bleached pigment activates transduction in isolated rods of the salamander retina. *Journal of Physiology* **480**, 261-279.

Cote RH, Bownds MD, & Arshavsky VY (1994). cGMP binding sites on photoreceptor phosphodiesterase: role in feedback regulation of visual transduction. *Proceedings of the National Academy of Sciences of the United States of America* **91**, 4845-4849.

Demontis GC, Gargini C, Paoli TG, & Cervetto L (2009). Selective Hcn1 channels inhibition by ivabradine in mouse rod photoreceptors. *Investigative Ophthalmology & Visual Science* **50**, 1948-1955.

Demontis GC, Longoni B, Barcaro U, & Cervetto L (1999). Properties and functional roles of hyperpolarization-gated currents in guinea-pig retinal rods. *Journal of Physiology* **515**, 813-828.

Demontis GC, Moroni A, Gravante B, Altomare C, Longoni B, Cervetto L, & DiFrancesco D (2002). Functional characterisation and subcellular localisation of HCN1 channels in rabbit retinal rod photoreceptors. *Journal of Physiology* **542**, 89-97.

Dizhoor AM, Olshevskaya EV, Henzel WJ, Wong SC, Stults JT, Ankoudinova I, & Hurley JB (1995). Cloning, sequencing, and expression of a 24-kDa Ca(2+)-binding protein activating photoreceptor guanylyl cyclase. *Journal of Biological Chemistry* **270**, 25200-25206.

Dizhoor AM, Olshevskaya EV, & Peshenko IV (2010). Mg2+/Ca2+ cation binding cycle of guanylyl cyclase activating proteins (GCAPs): role in regulation of photoreceptor guanylyl cyclase. *Molecular and Cellular Biochemistry* **334**, 117-124.

Doan T, Azevedo AW, Hurley JB, & Rieke F (2009). Arrestin competition influences the kinetics and variability of the single-photon responses of mammalian rod photoreceptors. *Journal of Neuroscience* **29**, 11867-11879.

Doering CJ, Peloquin JB, & McRory JE (2007). The Ca(v)1.4 calcium channel: more than meets the eye. *Channels (Austin)* **1**, 3-10.

Eisenman G & Horn R (1983). Ionic selectivity revisited: the role of kinetic and equilibrium processes in ion permeation through channels. *Journal of Membrane Biology* **76**, 197-225.

Fain GL, Lamb TD, Matthews HR, & Murphy RL (1989). Cytoplasmic calcium as the messenger for light adaptation in salamander rods. *Journal of Physiology* **416**, 215-243.

Fain GL, Quandt FN, Bastian BL, & Gerschenfeld HM (1978). Contribution of a caesium-sensitive conductance increase to the rod photoresponse. *Nature* **272**, 466-469.

Falke JJ, Drake SK, Hazard AL, & Peersen OB (1994). Molecular tuning of ion binding to calcium signaling proteins. *Quarterly Reviews of Biophysics* **27**, 219-290.

Falke JJ, Snyder EE, Thatcher KC, & Voertler CS (1991). Quantitating and engineering the ion specificity of an EF-hand-like Ca2+ binding. *Biochemistry* **30**, 8690-8697.

Fesenko EE, Kolesnikov SS, & Lyubarsky AL (1985). Induction by cyclic GMP of cationic conductance in plasma membrane of retinal rod outer segment. *Nature* **313**, 310-313.

Flaherty KM, Zozulya S, Stryer L, & McKay DB (1993). Three-dimensional structure of recoverin, a calcium sensor in vision. *Cell* **75**, 709-716.

Fu Y & Yau KW (2007). Phototransduction in mouse rods and cones. *Pflugers Archives* **454**, 805-819.

Furman RE & Tanaka JC (1990). Monovalent selectivity of the cyclic guanosine monophosphate- activated ion channel. *Journal of General Physiology* **96**, 57-82.

Gargini C, Demontis GC, Bisti S, & Cervetto L (1999). Effects of blocking the hyperpolarization-activated current (Ih) on the cat electroretinogram. *Vision Research* **39**, 1767-1774.

Gifford JL, Walsh MP, & Vogel HJ (2007). Structures and metal-ion-binding properties of the Ca2+-binding helix-loop-helix EF-hand motifs. *Biochemical Journal* **405**, 199-221.

Gorczyca WA, Gray-Keller MP, Detwiler PB, & Palczewski K (1994). Purification and physiological evaluation of a guanylate cyclase activating protein from retinal rods. *Proceedings of the National Academy of Sciences of the United States of America* **91**, 4014-4018.

Gouras P & MacKay CJ (1989). Growth in amplitude of the human cone electroretinogram with light adaptation. *Investigative Ophthalmology & Visual Science* **30**, 625-630.

Granit R (1933). The components of the retinal action potential in mammals and their relation to the discharge in the optical nerve. *Journal of Physiology* **77**, 207-239.

Green DG & Kapousta-Bruneau NV (1999). A dissection of the electroretinogram from the isolated rat retina with microelectrodes and drugs. *Visual Neuroscience* **16**, 727-741.

Gross OP & Burns ME (2010). Control of Rhodopsin's Active Lifetime by Arrestin-1 Expression in Mammalian Rods. *Journal of Neuroscience* **30**, 3450-3457.

Haeseleer F, Imanishi Y, Maeda T, Possin DE, Maeda A, Lee A, Rieke F, & Palczewski K (2004). Essential role of Ca(2+)-binding protein 4, a Ca(v)1.4 channel regulator, in photoreceptor synaptic function. *Nature Neuroscience* **7**, 1079-1087.

Hagins WA, Penn RD, & Yoshikami S (1970). Dark current and photocurrent in retinal rods. *Biophysical Journal* **10**, 380-412.

Hagins WA, Robinson WE, & Yoshikami S (1975). Ionic aspects of excitation in rod outer segments. *Ciba Foundation Symposium* 169-189.

Hamer RD, Nicholas SC, Tranchina D, Lamb TD, & Jarvinen JL (2005). Toward a unified model of vertebrate rod phototransduction. *Visual Neuroscience* **22**, 417-436.

Hamer RD, Nicholas SC, Tranchina D, Liebman PA, & Lamb TD (2003). Multiple steps of phosphorylation of activated rhodopsin can account for the reproducibility of vertebrate rod single-photon responses. *Journal of General Physiology* **122**, 419-444.

Haverkamp S, Grunert U, & Wassle H (2001). Localization of kainate receptors at the cone pedicles of the primate retina. *Journal of Comparative Neurology* **436**, 471-486.

Haynes LW, Kay AR, & Yau KW (1986). Single cyclic GMP-activated channel activity in excised patches of rod outer segment membrane. *Nature* **321**, 66-70.

He W, Cowan CW, & Wensel TG (1998). RGS9, a GTPase accelerator for phototransduction. *Neuron* **20**, 95-102.

Hestrin S (1987). The properties and function of inward rectification in rod photoreceptors of the tiger salamander. *Journal of Physiology* **390**, 319-333.

Hodgkin AL, McNaughton PA, & Nunn BJ (1985). The ionic selectivity and calcium dependence of the light- sensitive pathway in toad rods. *Journal of Physiology* **358**, 447-468.

Hodgkin AL, McNaughton PA, Nunn BJ, & Yau KW (1984). Effect of ions on retinal rods from Bufo marinus. *Journal of Physiology* **350**, 649-680.

Hsu YT & Molday RS (1993). Modulation of the cGMP-gated channel of rod photoreceptor cells by calmodulin. *Nature* **361**, 76-79.

Hughes BA, Kumar G, Yuan Y, Swaminathan A, Yan D, Sharma A, Plumley L, Yang-Feng TL, & Swaroop A (2000). Cloning and functional expression of human retinal kir2.4, a pH-sensitive inwardly rectifying K(+) channel. *American Journal of Physiology: Cell Physiology* **279**, C771-C784.

Jamison JA, Bush RA, Lei B, & Sieving PA (2001). Characterization of the rod photoresponse isolated from the dark-adapted primate ERG. *Visual Neuroscience* **18**, 445-455.

Kang Derwent JJ & Linsenmeier RA (2001). Intraretinal analysis of the a-wave of the electroretinogram (ERG) in dark-adapted intact cat retina. *Visual Neuroscience* **18**, 353-363.

Kaupp UB, Schnetkamp PP, & Junge W (1979). Light-induced calcium release in isolated intact cattle rod outer segments upon photoexcitation of rhodopsin. *Biochimica et Biophysica Acta* **552**, 390-403.

Kawai F, Horiguchi M, Suzuki H, & Miyachi E (2001). Na(+) action potentials in human photoreceptors. *Neuron* **30**, 451-458.

Kawai F, Horiguchi M, Suzuki H, & Miyachi E (2002). Modulation by hyperpolarization-activated cationic currents of voltage responses in human rods. *Brain Res* **943**, 48-55.

Kawamura S (1993). Rhodopsin phosphorylation as a mechanism of cyclic GMP phosphodiesterase regulation by S-modulin. *Nature* **362**, 855-857.

Kinjo TG, Szerencsei RT, Winkfein RJ, Kang K, & Schnetkamp PP (2003). Topology of the retinal cone NCKX2 Na/Ca-K exchanger. *Biochemistry* **42**, 2485-2491.

Klenchin VA, Calvert PD, & Bownds MD (1995). Inhibition of rhodopsin kinase by recoverin. Further evidence for a negative feedback system in phototransduction. *Journal of Biological Chemistry* **270**, 16147-16152.

Knop GC, Seeliger MW, Thiel F, Mataruga A, Kaupp UB, Friedburg C, Tanimoto N, & Muller F (2008). Light responses in the mouse retina are prolonged upon targeted deletion of the HCN1 channel gene. *European Journal of Neuroscience* **28**, 2221-2230.

Knopp A & Rüppel H (1996). Ca2+ fluxes and channel regulation in rods of the albino rat. *Journal of General Physiology* **107**, 577-595.

Koch KW & Stryer L (1988). Highly cooperative feedback control of retinal rod guanylate cyclase by calcium ions. *Nature* **334**, 64-66.

Kolb H & West RW (1977). Synaptic connections of the interplexiform cell in the retina of the cat. *J Neurocytol* **6**, 155-170.

Kourennyi DE, Liu X, & Barnes S (2002). Modulation of rod photoreceptor potassium Kx current by divalent cations. *Annals of Biomedical Engineering* **30**, 1196-1203.

Koutalos Y, Nakatani K, Tamura T, & Yau KW (1995). Characterization of guanylate cyclase activity in single retinal rod outer segments. *Journal of General Physiology* **106**, 863-890.

Krispel CM, Chen D, Melling N, Chen YJ, Martemyanov KA, Quillinan N, Arshavsky VY, Wensel TG, Chen CK, & Burns ME (2006). RGS expression rate-limits recovery of rod photoresponses. *Neuron* **51**, 409-416.

Krizaj D & Copenhagen DR (1998). Compartmentalization of calcium extrusion mechanisms in the outer and inner segments of photoreceptors. *Neuron* **21**, 249-256.

Kurenny DE & Barnes S (1994). Proton modulation of M-like potassium current (IKx) in rod photoreceptors. *Neuroscience Letters* **170**, 225-228.

Kuzmin DG, Travnikov SV, Firth SI, & Govardovskii V (2004). Mathematical Model and Light Adaptation in Frog Retinal Rods. *Sensory Systems* **18**, 305-316.

Lagnado L, Cervetto L, & McNaughton PA (1992). Calcium homeostasis in the outer segments of retinal rods from the tiger salamander. *Journal of Physiology* **455**, 111-142.

Lamb TD (1994). Stochastic simulation of activation in the G-protein cascade of phototransduction. *Biophysical Journal* **67**, 1439-1454.

Lamb TD & Matthews HR (1988). External and internal actions in the response of salamander retinal rods to altered external calcium concentration. *Journal of Physiology* **403**, 473-494.

Lamb TD & Pugh EN, Jr. (1992). A quantitative account of the activation steps involved in phototransduction in amphibian photoreceptors. *Journal of Physiology* **449**, 719-758.

Leeper HF & Copenhagen DR (1979). Mixed rod-cone responses in horizontal cells of snapping turtle retina. *Vision Research* **19**, 407-412.

Leskov IB, Klenchin VA, Handy JW, Whitlock GG, Govardovskii VI, Bownds MD, Lamb TD, Pugh ENJ, & Arshavsky VY (2000). The gain of rod phototransduction: reconciliation of biochemical and electrophysiological measurements. *Neuron* **27**, 525-537.

Li H, Chuang AZ, & O'Brien J (2009). Photoreceptor coupling is controlled by connexin 35 phosphorylation in zebrafish retina. *Journal of Neuroscience* **29**, 15178-15186.

Lipton SA, Ostroy SE, & Dowling JE (1977). Electrical and adaptive properties of rod photoreceptors in Bufo marinus. I. Effects of altered extracellular Ca2+ levels. *Journal of General Physiology* **70**, 747-770.

Liu XD & Kourennyi DE (2004a). Effects of tetraethylammonium on Kx channels and simulated light response in rod photoreceptors. *Annals of Biomedical Engineering* **32**, 1428-1442.

Liu XD & Kourennyi DE (2004b). Linear system analysis of ion channel modulation in rod photoreceptors under dim light conditions. *Conference Proceedings IEEE Engineering in Medicine and Biology Society* **6**, 4037-4040.

Lolley RN & Racz E (1982). Calcium modulation of cyclic GMP synthesis in rat visual cells. *Vision Research* **22**, 1481-1486.

Luo DG, Xue T, & Yau KW (2008). How vision begins: an odyssey. *Proceedings of the National Academy of Sciences of United States of America* **105**, 9855-9862.

Makino CL, Dodd RL, Chen J, Burns ME, Roca A, Simon MI, & Baylor DA (2004). Recoverin regulates light-dependent phosphodiesterase activity in retinal rods. *Journal of General Physiology* **123**, 729-741.

Malcolm AT, Kourennyi DE, & Barnes S (2003). Protons and calcium alter gating of the hyperpolarization-activated cation current (I(h)) in rod photoreceptors. *Biochimica et Biophysica Acta* **1609**, 183-192.

Mansergh F, Orton NC, Vessey JP, Lalonde MR, Stell WK, Tremblay F, Barnes S, Rancourt DE, & Bech-Hansen NT (2005). Mutation of the calcium channel gene Cacna1f disrupts calcium signaling, synaptic transmission and cellular organization in mouse retina. *Human Molecular Genetics* **14**, 3035-3046.

Matthews HR (1995). Effects of lowered cytoplasmic calcium concentration and light on the responses of salamander rod photoreceptors. *Journal of Physiology* **484**, 267-286.

Matthews HR, Cornwall MC, & Crouch RK (2001). Prolongation of actions of Ca2+ early in phototransduction by 9-demethylretinal. *Journal of General Physiology* **118**, 377-390.

Matthews HR & Fain GL (2001). A light-dependent increase in free Ca2+ concentration in the salamander rod outer segment. *Journal of Physiology* **532**, 305-321.

Matthews HR, Murphy RL, Fain GL, & Lamb TD (1988). Photoreceptor light adaptation is mediated by cytoplasmic calcium concentration. *Nature* **334**, 67-69.

Mendez A, Burns ME, Sokal I, Dizhoor AM, Baehr W, Palczewski K, Baylor DA, & Chen J (2001). Role of guanylate cyclase-activating proteins (GCAPs) in setting the flash sensitivity of rod photoreceptors. *Proceedings of the National Academy of Sciences of the United States of America* **98**, 9948-9953.

Menini A, Rispoli G, & Torre V (1988). The ionic selectivity of the light-sensitive current in isolated rods of the tiger salamander. *Journal of Physiology* **402**, 279-300.

Mills SL & Massey SC (1995). Differential properties of two gap junctional pathways made by AII amacrine cells [see comments]. *Nature* **377**, 734-737.

Morgans CW, Bayley PR, Oesch NW, Ren G, Akileswaran L, & Taylor WR (2005). Photoreceptor calcium channels: insight from night blindness. *Visual Neuroscience* **22**, 561-568.

Morigiwa K & Vardi N (1999). Differential expression of ionotropic glutamate receptor subunits in the outer retina. *Journal of Comparative Neurology* **405**, 173-184.

Moriondo A, Pelucchi B, & Rispoli G (2001). Calcium-activated potassium current clamps the dark potential of vertebrate rods. *European Journal of Neuroscience* **14**, 19-26.

Nachman-Clewner M, St JR, & Townes-Anderson E (1999). L-type calcium channels in the photoreceptor ribbon synapse: localization and role in plasticity. *Journal of Comparative Neurology* **415**, 1-16.

Nakatani K & Yau KW (1988a). Calcium and light adaptation in retinal rods and cones. *Nature* **334**, 69-71.

Nakatani K & Yau KW (1988b). Calcium and magnesium fluxes across the plasma membrane of the toad rod outer segment. *Journal of Physiology* **395**, 695-729.

Nelson R (1977). Cat cones have rod input: a comparison of the response properties of cones and horizontal cell bodies in the retina of the cat. *Journal of Comparative Neurology* **172**, 109-135.

Nikonov S, Engheta N, Pugh EN, Jr., & Pugh EN (1998). Kinetics of recovery of the dark-adapted salamander rod photoresponse. *Journal of General Physiology* **111**, 7-37.

Nikonov S, Lamb TD, & Pugh ENJ (2000). The role of steady phosphodiesterase activity in the kinetics and sensitivity of the light-adapted salamander rod photoresponse. *Journal of General Physiology* **116**, 795-824.

Nir I, Harrison JM, Haque R, Low MJ, Grandy DK, Rubinstein M, & Iuvone PM (2002). Dysfunctional light-evoked regulation of cAMP in photoreceptors and abnormal retinal adaptation in mice lacking dopamine D4 receptors. *Journal of Neuroscience* **22**, 2063-2073.

Nomura A, Shigemoto R, Nakamura Y, Okamoto N, Mizuno N, & Nakanishi S (1994). Developmentally regulated postsynaptic localization of a metabotropic glutamate receptor in rat rod bipolar cells. *Cell* **77**, 361-369.

Nymark S, Heikkinen H, Haldin C, Donner K, & Koskelainen A (2005). Light responses and light adaptation in rat retinal rods at different temperatures. *Journal of Physiology* **567**, 923-938.

Okawa H, Sampath AP, Laughlin SB, & Fain GL (2008). ATP consumption by mammalian rod photoreceptors in darkness and in light. *Current Biology* **18**, 1917-1921.

Otto-Bruc AE, Fariss RN, Van HJ, & Palczewski K (1998). Phosphorylation of photolyzed rhodopsin is calcium-insensitive in retina permeabilized by alpha-toxin. *Proceedings of the National Academy of Sciences of the United States of America* **95**, 15014-15019.

Owen WG & Torre V (1983). High-pass filtering of small signals by retinal rods. Ionic studies. *Biophysical Journal* **41**, 325-339.

Ozawa T, Fukuda M, Nara M, Nakamura A, Komine Y, Kohama K, & Umezawa Y (2000). How can Ca2+ selectively activate recoverin in the presence of Mg2+? Surface plasmon resonance and FT-IR spectroscopic studies. *Biochemistry* **39**, 14495-14503.

Pelucchi B, Grimaldi A, & Moriondo A (2008). Vertebrate rod photoreceptors express both BK and IK calcium-activated potassium channels, but only BK channels are involved in receptor potential regulation. *Journal of Neuroscience Research* **86**, 194-201.

Penn RD & Hagins WA (1969). Signal transmission along retinal rods and the origin of the electroretinographic a-wave. *Nature* **223**, 201-204.

Penn RD & Hagins WA (1972). Kinetics of the photocurrent of retinal rods. *Biophysical Journal* **12**, 1073-1094.

Pepperberg DR, Cornwall MC, Kahlert M, Hofmann KP, Jin J, Jones GJ, & Ripps H (1992). Light-dependent delay in the falling phase of the retinal rod photoresponse. *Visual Neuroscience* **8**, 9-18.

Peshenko IV & Dizhoor AM (2004). Guanylyl cyclase-activating proteins (GCAPs) are Ca2+/Mg2+ sensors: implications for photoreceptor guanylyl cyclase (RetGC) regulation in mammalian photoreceptors. *Journal of Biological Chemistry* **279**, 16903-16906.

Peshenko IV & Dizhoor AM (2007). Activation and Inhibition of Photoreceptor Guanylyl Cyclase by Guanylyl Cyclase Activating Protein 1 (GCAP-1): The Functional Role of Mg2+/Ca2+ Exchange in EF-hand Domains. *Journal of Biological Chemistry* **282**, 21645-21652.

Peshenko IV, Olshevskaya EV, Savchenko AB, Karan S, Palczewski K, Baehr W, & Dizhoor AM (2011). Enzymatic Properties and Regulation of the Native Isozymes of Retinal Membrane Guanylyl Cyclase (RetGC) from Mouse Photoreceptors. *Biochemistry*.

Picco C & Menini A (1993). The permeability of the cGMP-activated channel to organic cations in retinal rods of the tiger salamander. *Journal of Physiology* **460**, 741-758.

Prinsen CF, Cooper CB, Szerencsei RT, Murthy SK, Demetrick DJ, & Schnetkamp PP (2002). The retinal rod and cone Na+/Ca2+-K+ exchangers. *Advances in Experimental Medicine & Biology* **514**, 237-251.

Pugh EN, Jr., Duda T, Sitaramayya A, & Sharma RK (1997). Photoreceptor guanylate cyclases: a review. *Bioscience Reports* **17**, 429-473.

Pugh EN, Jr., Falsini B, & Lyubarsky AL (1998). The origin of the major rod- and cone-driven components of the rodent electroretinogram, and the effect of age and light-rearing history on the magnitude of these components. In *Photostasis and Related Topics*, eds. Williams TP & Thistle AB, pp. 93-128. Plenum Press, New York.

Pugh EN, Jr. & Lamb TD. Phototransduction in vertebrate rods and cones: molecular mechanisms of amplification, recovery and light adaptation. In "Molecular Mechanisms in Visual Transduction". Stavenga, D. G., DeGrip, W. J., and Pugh, E. N. Jr. First ed.[3], 183-255. 2000. Amsterdam, Elsevier. Handbook of Biological Physics.

Raviola E & Gilula NB (1973). Gap junctions between photoreceptor cells in the vertebrate retina. *Proceedings of the National Academy of Sciences of the United States of America* **70**, 1677-1681.

Rebrik TI & Korenbrot JI (2004). In intact mammalian photoreceptors, Ca2+-dependent modulation of cGMP-gated ion channels is detectable in cones but not in rods. *Journal of General Physiology* **123**, 63-75.

Reilander H, Achilles A, Friedel U, Maul G, Lottspeich F, & Cook NJ (1992). Primary structure and functional expression of the Na/Ca,K- exchanger from bovine rod photoreceptors. *EMBO Journal* **11**, 1689-1695.

Ribelayga C, Cao Y, & Mangel SC (2008). The circadian clock in the retina controls rod-cone coupling. *Neuron* **59**, 790-801.

Ribelayga C & Mangel SC (2010). Identification of a circadian clock-controlled neural pathway in the rabbit retina. *PLoS ONE* **5**, e11020.

Rieke F & Schwartz EA (1994). A cGMP-gated current can control exocytosis at cone synapses. *Neuron* **13**, 863-873.

Rieke F & Schwartz EA (1996). Asynchronous transmitter release: control of exocytosis and endocytosis at the salamander rod synapse. *Journal of Physiology* **493**, 1-8.

Robson & Frishman (2011). The A-wave of the Electroretinogram: Importance of Axonal Currents. ARVO Meeting Abstracts 52:692

Savchenko A, Barnes S, & Kramer RH (1997). Cyclic-nucleotide-gated channels mediate synaptic feedback by nitric oxide. *Nature* **390**, 694-698.

Schmitz Y & Witkovsky P (1997). Dependence of photoreceptor glutamate release on a dihydropyridine-sensitive calcium channel. *Neuroscience* **78**, 1209-1216.

Schneeweis DM & Schnapf JL (1995). Photovoltage of rods and cones in the macaque retina. *Science* **268**, 1053-1056.

Schneider BG, Shyjan AW, & Levenson R (1991). Co-localization and polarized distribution of Na,K-ATPase alpha 3 and beta 2 subunits in photoreceptor cells. *Journal of Histochemistry and Cytochemistry* **39**, 507-517.

Schnetkamp PP (1980). Ion selectivity of the cation transport system of isolated intact cattle rod outer segments: evidence for a direct communication between the rod plasma membrane and the rod disk membranes. *Biochimica et Biophysica Acta* **598**, 66-90.

Schnetkamp PP (1991). Optical measurements of Na-Ca-K exchange currents in intact outer segments isolated from bovine retinal rods. *Journal of General Physiology* **98**, 555-573.

Schnetkamp PP (1995a). Calcium homeostasis in vertebrate retinal rod outer segments. *Cell Calcium* **18**, 322-330.

Schnetkamp PP (1995b). How does the retinal rod Na-Ca+K exchanger regulate cytosolic free Ca2+? *Journal of Biological Chemistry* **270**, 13231-13239.

Schnetkamp PP & Szerencsei RT (1991). Effect of potassium ions and membrane potential on the Na-Ca-K exchanger in isolated intact bovine rod outer segments. *Journal of Biological Chemistry* **266**, 189-197.

Schwartz EA (1981). First events in vision: the generation of responses in vertebrate rods. *Journal of Cell Biology* **90**, 271-278.

Stephen R, Bereta G, Golczak M, Palczewski K, & Sousa MC (2007). Stabilizing function for myristoyl group revealed by the crystal structure of a neuronal calcium sensor, guanylate cyclase-activating protein 1. *Structure* **15**, 1392-1402.

Stern JH, Knutsson H, & MacLeish PR (1987). Divalent cations directly affect the conductance of excised patches of rod photoreceptor membrane. *Science* **236**, 1674-1678.

Tanaka T, Ames JB, Harvey TS, Stryer L, & Ikura M (1995). Sequestration of the membrane-targeting myristoyl group of recoverin in the calcium-free state. *Nature* **376**, 444-447.

Thoreson WB, Bryson EJ, & Rabl K (2003). Reciprocal interactions between calcium and chloride in rod photoreceptors. *Journal of Neurophysiology* **90**, 1747-1753.

Thoreson WB, Nitzan R, & Miller RF (2000). Chloride efflux inhibits single calcium channel open probability in vertebrate photoreceptors: chloride imaging and cell-attached patch-clamp recordings. *Visual Neuroscience* **17**, 197-206.

Torre V, Matthews HR, & Lamb TD (1986). Role of calcium in regulating the cyclic GMP cascade of phototransduction in retinal rods. *Proceedings of the National Academy of Sciences of the United States of America* **83**, 7109-7113.

Tsang SH, Burns ME, Calvert PD, Gouras P, Baylor DA, Goff SP, & Arshavsky VY (1998). Role for the target enzyme in deactivation of photoreceptor G protein in vivo. *Science* **282**, 117-121.

Tsukamoto Y, Morigiwa K, Ueda M, & Sterling P (2001). Microcircuits for night vision in mouse retina. *Journal of Neuroscience* **21**, 8616-8623.

Wilden U, Hall SW, & Kuhn H (1986). Phosphodiesterase activation by photoexcited rhodopsin is quenched when rhodopsin is phosphorylated and binds the intrinsic 48-kDa protein of rod outer segments. *Proceedings of the National Academy of Sciences of the United States of America* **83**, 1174-1178.

Woodruff ML, Janisch KM, Peshenko IV, Dizhoor AM, Tsang SH, & Fain GL (2008). Modulation of phosphodiesterase6 turnoff during background illumination in mouse rod photoreceptors. *Journal of Neuroscience* **28**, 2064-2074.

Woodruff ML, Olshevskaya EV, Savchenko AB, Peshenko IV, Barrett R, Bush RA, Sieving PA, Fain GL, & Dizhoor AM (2007). Constitutive excitation by Gly90Asp rhodopsin rescues rods from degeneration caused by elevated production of cGMP in the dark. *Journal of Neuroscience* **27**, 8805-8815.

Woodruff ML, Sampath AP, Matthews HR, Krasnoperova NV, Lem J, & Fain GL (2002). Measurement of cytoplasmic calcium concentration in the rods

of wild-type and transducin knock-out mice. *Journal of Physiology* **542**, 843-854.

Xin D & Bloomfield SA (1999). Dark- and light-induced changes in coupling between horizontal cells in mammalian retina. *Journal of Comparative Neurology* **405**, 75-87.

Xu J, Dodd RL, Makino CL, Simon MI, Baylor DA, & Chen J (1997). Prolonged photoresponses in transgenic mouse rods lacking arrestin. *Nature* **389**, 505-509.

Xu JW & Slaughter MM (2005). Large-conductance calcium-activated potassium channels facilitate transmitter release in salamander rod synapse. *Journal of Neuroscience* **25**, 7660-7668.

Yagi T & MacLeish PR (1994). Ionic conductances of monkey solitary cone inner segments. *Journal of Neurophysiology* **71**, 656-665.

Yamazaki A, Sen I, Bitensky MW, Casnellie JE, & Greengard P (1980). Cyclic GMP-specific, high affinity, noncatalytic binding sites on light-activated phosphodiesterase. *Journal of Biological Chemistry* **255**, 11619-11624.

Yau KW & Hardie RC (2009). Phototransduction motifs and variations. *Cell* **139**, 246-264.

Yau KW, McNaughton PA, & Hodgkin AL (1981). Effect of ions on the light-sensitive current in retinal rods. *Nature* **292**, 502-505.

Yau KW & Nakatani K (1984). Electrogenic Na-Ca exchange in retinal rod outer segment. *Nature* **311**, 661-663.

Zhong H, Molday LL, Molday RS, & Yau KW (2002). The heteromeric cyclic nucleotide-gated channel adopts a 3A:1B stoichiometry. *Nature* **420**, 193-198.

Aalto-DD 67/2011

ISBN 978-952-60-4235-0 (pdf)
ISBN 978-952-60-4234-3
ISSN-L 1799-4934
ISSN 1799-4942 (pdf)
ISSN 1799-4934

Aalto University
School of Science
Department of Biomedical Engineering and Computational Science

BUSINESS + ECONOMY

ART + DESIGN + ARCHITECTURE

SCIENCE + TECHNOLOGY

CROSSOVER

DOCTORAL DISSERTATIONS